

Response to Referee #1

1
2
3
4
5
6
7
8
9
10
11
12
13
14
15
16
17
18
19
20
21
22
23
24
25
26
27
28
29

With the development of social economy and population density increases, evidences have indicated that land use and environmental quality change a lot at a global scale, and the surface ecosystem becomes increasingly fragile. The surface vegetation cover has serious deteriorated by multi-sources (including NOAA-AVHRR and TIROS-TOVS satellite remote sensing data), which has been largely documented. While land cover changes, land variables such as albedo, roughness, and bulk transfer coefficients, also change, which lead to the variation of surface heat fluxes, and then result in surface temperature anomaly. Therefore, in many previous studies, using dramatic land condition change to evaluate the land surface process impact has been widely used for regional land surface impact studies in preliminary stage to excite more comprehensive studies. And most of them focused on the importance of land surface processes through climate modeling. This research investigated the impacts of different surface parameters for four different surface types over the mid-to-lower reaches of Yangtze River on the radiation budget and surface-atmosphere water, heat and mass exchanges. Firstly, the authors revealed the differences in several physical parameters among the four typical surface types. Secondly, they tried to explore the mechanism for the differences. The analyses in the paper are well organized and the results are reasonable. Few published papers discuss the differences of surface physical parameters among different surface types based on the field observations, especially over the mid-to-lower reaches of Yangtze River Valley. This paper provides useful information, especially for the land-atmospheric interaction research over East Asia monsoon region. The presentation of this article is generally clear. I suggest publication of this paper with some revisions.

Response: We would like to thank the referee for providing the insightful suggestions, which indeed help us reconsider and further explore the underlying problems in comparing the land-atmosphere interaction at different surface types in the mid-to-lower Yangtze River valley. In the revised manuscript, we have added more descriptions on the research background and in-depth discussion of the differences in micro-climate elements and mechanism analysis.

Major comments:

1 • *In the first part of the introduction, the authors review many studies about the impacts of*
2 *land cover change on global and regional climate. Land-atmosphere interaction is strong in*
3 *East Asian monsoon zone. Since the research focus on Yangtze River, some previous work on*
4 *LULCC effects on China or East Asian climate should be mentioned importantly in the*
5 *introduction. Actually, there were serious land degradations over East Asia during the past*
6 *several decades and have identified Tibet Plateau, Northwest China and Inner Mognial were*
7 *among areas with severe land degradation. For example, Xue et al. (1996) and Qian and Xue*
8 *(2010) have pointed out the East Asia summer monsoon circulation was weakened and the*
9 *precipitation is reduced due to the land degradation over three areas.*

10 **Response:** Accepted. The references of previous work on LULCC effects on East Asia has
11 been added in the introduction in the revised manuscript (P4, lin14-17).

12

13 • *In Table 1, the units of the measurement height for soil temperature and water content are*
14 *not specified. It should be cm? Please complete them.*

15 **Response:** We have added the units of the measurement height for soil temperature and water
16 content, it's "cm" in Table 1.

17

18 • *In page 10, line 10 and 11, “....., and it also lags in the summer that in the spring ”*
19 *please clarify the sentence. It's so hard for readers to understand. Also, in the same line,*
20 *“Due to the influence of the surface,..... ”, it's a general statement and in the research*
21 *article, it should be avoided. It's better to state what the influences are and how the surface*
22 *or other anthropogenic factors make the surface temperature show larger diurnal range than*
23 *air temperature.*

24 **Response:** Thanks. We rephrased the sentence “*and it also lags in the summer that in the*
25 *spring ”* as “ *The peak time of both air and surface temperature in spring lags that in*
26 *summer.*” in P10, line 11-13. Besides, the difference of radiation budget on land surface
27 between daytime and nighttime results in larger diurnal range of surface temperature than air
28 temperature. The words “*Due to the influence of the surface*” was unclear for readers to
29 understand, so we rewrote it in P10, line 28-29.

1
2
3
4
5
6
7
8
9
10
11
12
13
14
15
16
17
18
19
20
21
22
23
24
25
26
27

• *In the results and discussion part, the authors show the differences of many observed elements and several surface characteristics over four sites during spring and summer. Actually, tables that can show the detailed quantitative differences could be the compliment for the figures (e.g. figure 2, figure 3.....). For example, for the figure 3, a table can be presented that show the average of diurnal air temperature, surface temperature and relative humidity for the four sites. The table and figure can exhibit the differences more easily observable.*

Response: Accepted. Figure 2 has already shown the average of micro-meteorological elements for the four sites in different season, and we added the diurnal range of these elements below figure 2 in the revised manuscript.

1

2

Response to Referee #2

3

4 *The comparison studies for data analysis from paired observational sites under same (or*
5 *similar) climate background could reveal the differences of energy budgets which resulted by*
6 *land surface characteristics directly and quantitatively. The mid- to lower reaches of Yangtze*
7 *Rivers is located within the East Asia Monsoon zone, and the mechanism of LULCC is*
8 *complicated because of the interaction between the general circulation and human activities.*
9 *The four surface types selected in this study are the most typical in the region. The paper is*
10 *well organized and written, I suggest it will be published after some revision.*

11 **Response:** We would like to appreciate the referee for providing the insightful suggestions,
12 which indeed help us reconsider and further explore the the differences of land-atmosphere
13 interaction at different surface types in the mid-to-lower Yangtze River valley. In the revised
14 manuscript, we have added more clear descriptions on the location of the pair sites and
15 comparison on physical characteristics with different land cover, as well as in-depth
16 discussion concerning the mechanism.

17

18 *Major comments:*

19 • *A subplot is suggested to be added in Fig1, which content the location of 4 sites with*
20 *satellite background. It will be better understanding than written-description.*

21 **Response:** Thanks. We have added the subplot in Figure 1. It will be easier for readers to
22 know the location and surface types.

23

24 • *I also suggest the DX and XL are replaced by DX_urban and XL_suburb.*

25 **Response:** Accepted. “DX” and “XL” have been replaced by “DX-urban” and “XL-suburb”
26 in the revised manuscript.

27

1 • In P12, L1-2, this sentence should be present in part 2.3.1, after the variables description. Is
2 there any more QA/QC consideration for eddy covariance data processes?

3 **Response:** We rechecked the sentence in P12, line1-2, and there may be some
4 misunderstandings. QA/QC is definitely a crucial issue for the proper use of eddy covariance
5 data. In section 2.2, the QA/QC is mentioned as follows: “Strict correction and quality control
6 (Foken et al., 2004) have been performed for all the turbulence measurements. Coordinate
7 rotation correction (Wilczak et al., 2001), frequency response correction (Moore, 1986), and
8 WPL correction etc. are applied in this study.”

9

10 • The approximate irrigation schedule should introduce in the part of LS_crop site description;

11 **Response:** We have added the schedule of agricultural activities in the part of LS-crop site
12 description in the part of LS-crop site description in P6, line 11-13.

13

14 • In Fig 11. There exist obvious high correlation between albedo and precipitation for
15 LS_crop and DX sites and low correlation between LS_grass and XL sites, I suggest the
16 authors give some interpretation.

17 **Response:** It is human activities that results in the high correlation between albedo and
18 precipitation for LS-crop and DX-urban sites but not for LS-grass or XL-suburb sites. At
19 urban site, roof of the building is nearly watertight, the waterlogging after raining leads to a
20 high albedo in a short time. In cropland, the soil with sparse vegetation cover has high soil
21 wetness during the growing season. When being covered by water after rainfall event, the
22 albedo increases immediately. This phenomenon has been explained in the part of 3.3.1.

23

24 • Page 16, L9-10, the variation for RH is mainly affected by synoptic system, it is hard to
25 depict it varies with the Bowen ration and temperature.

26 **Response:** Accepted. We rewrote this sentence in the revised manuscript. The variation of
27 RH is not attributed only to vertical turbulent exchange, but also advection. Temperature and
28 water vapor can not fully explain the change of RH in P16, line 18-23.

29

Response to Short Comment from Scientific Community #1

This manuscript revealed the differences of land-atmosphere interactions in four typical land cover types (Urban surface, Suburban surface, Grassland surface and Cropland surface). It is well organized and written. I suggest this manuscript for publication in Atmospheric Chemistry and Physics after some minor revisions and corrections.

Response: We would like to thank the referee for providing the insightful comments, which indeed help us reconsider and further explore the underlying problems when we analyze the difference of land-atmosphere interaction at different surface types in the mid-to-lower Yangtze River valley. In the revised manuscript, we have added more clear descriptions on the physical characteristics of climate elements and surface parameter, as well as the discussion of mechanism.

General comments:

- *DX-Urban and XL-Suburb terms in the manuscript are suggested to replace corresponding DX and XL terms, and then land cover type will be distinguished more easily like LS-crop and LS-grass terms.*

Response: Accepted. These replacements help the readers more easily to understand.

- *Nighttime surface/air temperature differences are mainly emphasized in the manuscript, but day time surface/air temperature differences are rarely discussed. From Figure 3, we can see that daytime urban site surface/air temperature is lower than suburb site or grass site, it is just the opposite of the existing results based on remote sensing LST data and meteorological station data, extra explanations or discussions about the contrary daytime surface/air temperature results are needed in this paper. Following existing publications are recommended for reference:*

1 Liu, S., Jiang, R., Wang C. Wang Y.: Observation analysis on spatial and temporal
2 distribution characteristics of summer urban heat island in Nanjing (in Chinese), *Trans*
3 *Atmos Sci*, 37(1): 19-27, 2014

4 Zeng, Y., Qiu, X. F., Gu, L. H., He, Y. J., Wang, K. F.: The urban heat island in Nanjing,
5 *Quaternary International*, 208(1), 38-43, 2009.

6 Zhou, D., Zhao, S., Liu, S., Zhang, L., Zhu, C.: Surface urban heat island in China ' s 32
7 major cities: Spatial patterns and drivers, *Remote Sensing of Environment*, 152, 51-61, 2014.

8 **Response:** Firstly, as the first paper mentioned, UHI is evident in the nighttime but not
9 typical in the daytime. Secondly, when discussing the intensity of UHI, we must take the
10 climate background into consideration. As shown in the figure below, summer in 2013 is an
11 extremely drought period in southern China, the precipitation decreased by more than 78% of
12 the average amount, breaking the historical record over the past 50 years (Yuan et al., 2016),
13 especially in the mid-to-lower reaches of Yangtze River (Hou et al, 2014; Zhao et al., 2015).
14 We therefore have an assumption to explain the “contradictory” phenomenon mentioned
15 above. In the urban area and cropland, human watering and irrigation or other activities
16 alleviate the natural drought effect in these areas. But in the grassland and suburb area,
17 lacking water limited evaporation cooling to a large extent. So the extreme drought induced
18 higher temperature in the natural vegetation cover in 2013 than before but didn't have large
19 influence in the area with intense human activities, and therefore not only weakened UHI but
20 also made daytime urban site surface/air temperature lower than suburb site or grass site.

21

22 Reference

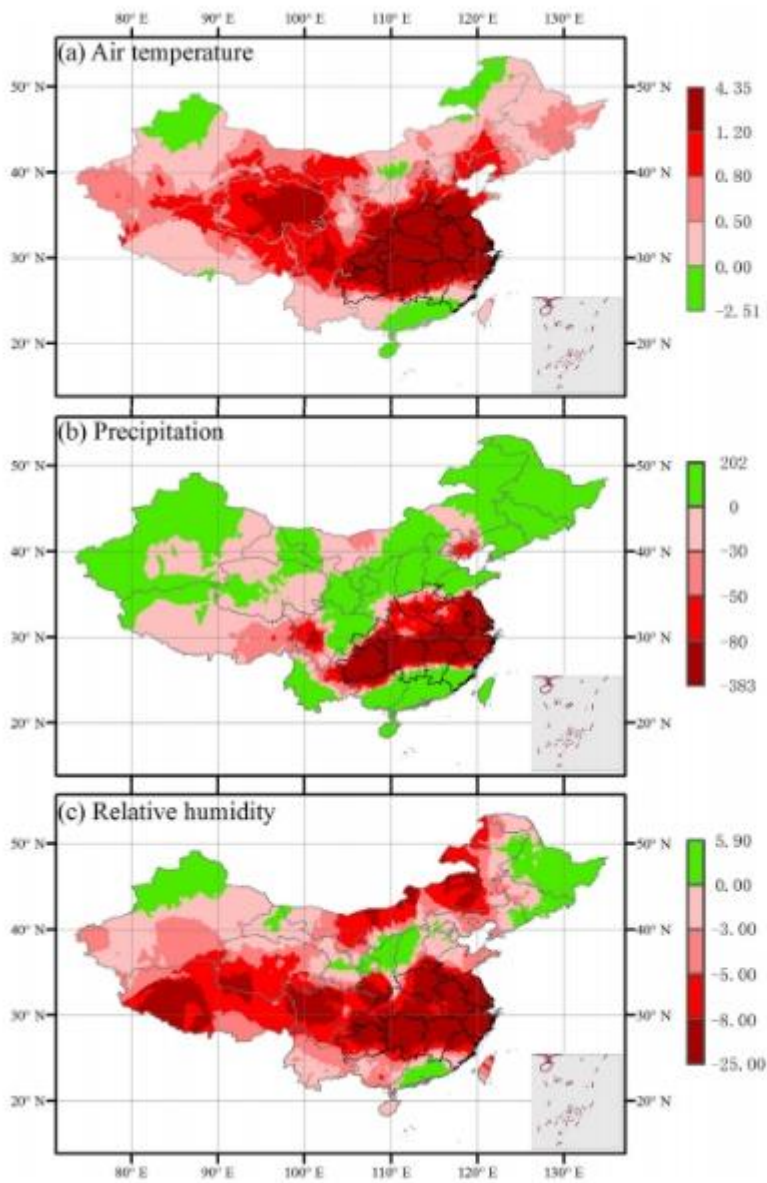
23 Hou W, Chen Y, Li Y, et al. Climatic characteristics over China in 2013 [J].

24 *Meteorological Monthly*, 2014, 40(4):482-493 (in Chinese).

25 Yuan W, Cai W, Yang C, et al. Severe summer heatwave and drought strongly
26 reduced carbon uptake in Southern China [J]. *Scientific Reports*, 2016, 6(25):87–90.

27 Zhao J, Yang J, Gong Z, et al. Analysis of and Discussion about Dynamic-Statistical
28 Climate Prediction for Summer Rainfall of 2013 in China[J]. *Advances in*
29 *Meteorological Science & Technology*, 2015 (in Chinese).

30



1
2
3
4
5
6
7
8
9

Figure 1. Regional anomalies of air temperature (°C) (a), precipitation (mm) (b) and relative humidity (%) (c) during July-August 2013. All data compare 2013 and the average of 1960 – 2012. The provinces with bold black boundary lines are the study area in this study. The right-bottom figures show the boundary of South China Sea. The maps were created by the ArcMap 9.3. (Yuan et al., 2016)

1 • *Similar descriptions or explanations such as “albedo decrease with the growing of*
2 *vegetation” are mentioned in the manuscript many times, for example: Page15, line23,*
3 *line9-10 and line12-14, etc. It is not appropriate for this paper in my opinion. Firstly, it can*
4 *be seen that albedo increase with growing of the paddy rice from Figure 11, and this fact is*
5 *mentioned in Page15, line5-7. Secondly, relations between albedo and vegetation fraction is*
6 *not fixed, albedo may increase with the growing of vegetation according to existed studies.*
7 *Therefore, descriptions or explanations such as “albedo decrease with the growing of*
8 *vegetation” should be used with caution in order to avoid misleading the readers. Please*
9 *refer the following papers:*

10 *Gao, F.: MODIS bidirectional reflectance distribution function and albedo Climate*
11 *ModelingGridproductsandthevariabilityofalbedoformajorglobalvegetationtypes. Journal of*
12 *Geophysical Research, 110, D01104, 2005.*

13 *Rechid, D., Raddatz, T.J., Jacob, D.: Parameterization of snow-free land surface albedo as a*
14 *function of vegetation phenology based on MODIS data and applied in climate modelling.*
15 *Theoretical and Applied Climatology, 95, 245-255, 2009.*

16 *Wang, K., Liang, S., Schaaf, C. L., Strahler, A. H.: Evaluation of Moderate Resolution*
17 *Imaging Spectroradiometer land surface visible and shortwave albedo products at FLUXNET*
18 *sites. Journal of Geophysical Research, 115, D17107, 2010.*

19 **Response:** Thanks. The words “*albedo decrease with the growing of vegetation*” and
20 “*albedo always decreases with the increase of vegetation cover fraction*” is easy to mislead
21 the readers. We have rewritten it as “ Fig. 12 shows that except for XL-suburb site, the albedo
22 at the other three sites decrease from spring to summer. At the XL-suburb site with sparse and
23 low grass, possibly because of insufficient precipitation after mid-July, the summer albedo
24 increases and becomes slightly larger than that in the spring. But at grassland, the albedo
25 decreases largely in the green-up phrase, which results in the lower albedo in summer. And
26 the dramatic decrease of surface albedo in early June is associated with the biomass burning
27 due to the cultivation system in this region, i.e., a rotation of wheat in winter and rice in
28 summer.” in part of 3.3.1.

29

1 *Specific comments:*

2 • *Page11, line19: USR should be DLR, USR is affected by albedo, not clouds and aerosols in*
3 *the atmosphere.*

4 **Response:** It has been corrected in P11, line 26.

5

6 • *Page12, line15-18: It is hard to understand USR at the LS-crop site is smaller in the summer*
7 *than in the spring as a result of albedo increase(line17-18), I think it is a mistake. The*
8 *phenomenon that albedo at the LS-crop site in summer is smaller than that in spring can be*
9 *seen clearly in Figure 12. The sentence “where surface albedo increases in the summer due*
10 *to the decreased vegetation cover fraction” is also hard to understand, because vegetation*
11 *cover fraction is supposed to increase with the paddy rice growing in summer, please explain*
12 *this sentence more.*

13 **Response:** We corrected it in the part of 3.2.1. Yes, it is easy to misunderstand the sentence
14 that “*the maximum daily average USR at the LS-crop site is smaller in the summer than in the*
15 *spring by 16.98 Wm⁻², where surface albedo increases in the summer due to the decreased*
16 *vegetation cover fraction”*. Consider the seasonal variation, the decrease of albedo (Figure
17 12a) result in the decrease of USR (Figure 6c) at crop site from spring to summer. When it
18 comes to the daily variation, albedo increases from June to August in P12, line 20-26.

19

20 • *Page12, line18-19: The meaning of the sentence “As a result, the USR decreases by 90.35*
21 *,84.79,59.49 W m⁻² at the LS-crop, XL, and DX sites respectively.” is apparently not*
22 *corresponding to the Figure 6c, and LS-crop should be LS-grass because LS-crop is analyzed*
23 *before. At LS-grass, XL and DX sites, USR all increases? Please confirm it.*

24 **Response:** Corrected. We have rewrote this sentence as “USR at XL-suburb, LS-grass and
25 DX-urban grows to 90.35、84.79、59.49 W m⁻² respectively in the summer.” in P12, line 19-
26 20 in our revised manuscript.

27

- 1 • *Page16, line19-22: roughness lengths are not right according to Figure 13 and Figure 14,*
- 2 *please change “0.05m, 0.02m,and 0.17m ” to “0.02m, 0.05m,and 0.17m ” .*
- 3 **Response:** Accepted. It has been changed.

Comparison of land-atmosphere interaction at different surface types in the mid- to lower reaches of Yangtze River Valley

W.D. Guo^{1,2*}, X.Q. Wang^{1,2}, J.N. Sun^{1,2*}, A.J. Ding^{1,2}, and J. Zou^{1,2}

[1]{Institute for Climate and Global Change Research, School of Atmospheric Sciences, Nanjing University, Nanjing, China}

[2]{[Joint International Research Laboratory of Atmospheric and Earth System Sciences, Nanjing, China](#)}

[*]{Institute for Climate and Global Change Research, School of Atmospheric Sciences, Nanjing University, Nanjing, China}

Correspondence to: W.D. Guo (guowd@nju.edu.cn), or J.N. Sun (jnsun@nju.edu.cn)

Abstract

The mid- to lower reaches of Yangtze River Valley is located within the typical East Asia monsoon zone. Rapid urbanization, industrialization, and development of agriculture have led to fast and complicated land use and land cover changes in this region. To investigate land-atmosphere interaction in this region where human activities and monsoon climate are highly interactive with each other, micro-meteorological elements over four [sites with different surface types around Nanjing, including i.e. urban surface t Dangxiaorepresented by the observational site at Communist Party School in Nanjing](#) (hereafter [DX-urban](#)), suburban surface [represented by the ground site](#) at Xianling ([XL-suburb](#)), and grassland and farmland [represented by field sites](#) at Lishui County (LS-grass and LS-crop), are analyzed and their differences are revealed. [The i](#)mpacts of [different](#) surface parameters [ofapplied for](#) different surface types on the radiation budget and [land](#) surface-atmosphere heat, water, and mass exchanges are [investigated and comparedinvestigated](#). Results indicate that (1) the largest differences in daily average surface air temperature (T_a), surface skin temperature (T_s), and relative humidity (RH), which are found during the dry periods between [DX-urban](#) and LS-crop, can be up to 3.21°C, 7.26°C, and 22.79% respectively. [TDuring the growing season, the](#)

1 diurnal ranges of the above three elements are the smallest at DX-urban and the largest at LS-
2 grass, XL-suburb and LS-crop; (2) differences in radiative fluxes are mainly reflected in
3 upward shortwave radiation (USR) that is related to surface albedo and upward longwave
4 radiation (ULR) that is related to T_s . When comparing four sites, it can be found that both the
5 smallest USR and the largest ULR occur at DX-urban site. ~~USR is the smallest and ULR is the~~
6 ~~largest at DX-urban.~~ During the growing season, the average difference in ULR between the
7 ~~DX-urban site and other sites with vegetation cover can be up to 20Wm^{-2} .~~ The USR
8 ~~variability is the largest at LS-crop, while the~~ diurnal variation of ULR is ~~the~~ same as that of
9 T_s at all the four sites; (3) the differences in daily average sensible heat (H) and latent heat
10 (LE) between DX-urban and LS-crop are larger than 45 and 95Wm^{-2} , respectively. The
11 proportion of latent heat flux in the net radiation (LE/R_n) keeps increasing with the change of
12 season from the spring to summer; ~~XL-suburb site demonstrates a distinct forest feature;~~ (4)
13 ~~human activities have obvious effects on micro-climate. surface albedo is small while the~~
14 ~~Bowen ratio is large at DX-urban (an urban site). The U~~urban heat island effect results in
15 ~~higher T_a —is 2°C higher T_a at urban site than that at other sites in the nighttime. At crop site,~~
16 ~~It is found that surface albedo and roughness length variability both increase at LS-crop~~
17 ~~during the harvest season and straw burning periods.~~ LE is dominant due to irrigation ~~and n~~;
18 ~~Negative H is observed since evaporation cooling leads to low T_s . Daily variability of T_s is the~~
19 ~~lowest at LS-crop while RH is the largest At.~~ In the summer, the grassland albedo at XL-
20 suburb site gradually becomes larger than that at the sites in Lishui. Since the forest-like
21 ~~effects becomes more distinct at XL-suburb, LE/R_n increases rapidly. Thereby, although T_s is~~
22 higher at XL-suburb than that at LS-grass, there is no large difference in T_a between the two
23 sites due to the distinct effects of the planted forest.

25 1 Introduction

26 Land use/Land cover change (LULCC) is one of the most important anthropogenic forces to
27 weather and climate change in local, regional and global scale (IPCC, 2013). On earth, over
28 80% of the total land surface has been affected by human activities (Sanderson, 2002) in the
29 form of construction and farmland and loss of forest, and are increasing greatly at multiple
30 spatial and temporal scales in regions of different climate regimes. (Davin and De Noblet-
31 Ducoudré, 2010; Kalnay and Cai, 2003; Lawrence et al., 2012). Logging and creation of new
32 farmlands have changed land use in the tropics (DeFries et al., 2002); intensive human

1 activities in temperate regions have changed forests and grasslands to farmlands, while
2 urbanization and industrialization has been intensifying all the time and desert area has been
3 expanding (Gao et al., 2003; Suh and Lee, 2004). In boreal regions, forests have degraded to
4 grasslands and farmlands due to fire and pests damages as well as logging (Brown et al., 2010;
5 Lohila et al., 2010).

6 Under the same climate background, the radiation components and surface energy distribution
7 are controlled by characteristic surface factors such as vegetation cover, albedo, roughness
8 length, etc. (Amiro et al., 2006; Feddema et al., 2005; Jin and Roy, 2005), and subsequently
9 affect micro-meteorological elements of temperature, humidity, and precipitation. The effect
10 of LULCC on regional and global climate has been documented through the climate models.
11 Large-scale vegetation degradation and the development of agriculture and animal husbandry
12 in different scale will lead to decreases in precipitation (Mcalpine et al., 2009; Werth and
13 Avissar, 2002), while LULCC will affect the temperature difference between the surface and
14 air temperature and vegetation feedback ,such as tropical warming and boreal cooling due to
15 deforestation and urban heat island (Arnfield, 2003; Bounoua et al., 2002; Luysaert et al,
16 2014; Pielke et al., 2002).

17 However, a severe uncertainty in models still exists due to the insufficient knowledge of the
18 surface-atmosphere interaction in response to variations in surface fluxes and energy balance
19 (Bonan, 2008; Wang and Eleuterio, 2001; Pitman et al., 2009).One way to solve this problem
20 is verify the model and parameterization schemes by driving them with field measurement
21 and observations, which is really important in present study. With the development of a new
22 tool, Fluxnet (Baldocchi, 2001), a large number of land surface pair sites were built up from
23 wild, rural to urban and produce many significant results. Both management on existing types
24 of land cover and conversion to a different type can affect the local climate (Baldocchi, 2014).
25 The areodynamically rougher and darker oak savanna has higher R_n , H and T_a than the
26 grassland in the same climate condition (Baldocchi and Ma, 2013; Baldocchi et al, 2004);
27 deforestation would have a cooling effect on T_a in mid- to high latitudes and a warming effect
28 in low latitude (Lee et al., 2011); Wildfires on different land cover make different effects
29 (Krishman et al., 2012; Montes-Helu et al., 2009); the management practices of rangeland and
30 cropland or the change of crop types can influence the energy balance and water budget
31 (Alberto et al., 2009; Alberto et al.,2011; Baldocchi and Rao, 1995; Coulter et al., 2006;
32 Masseroni et al., 2014). Besides, in a city, LE at residential site is less dependent on short-

1 term precipitation that at grass site and H is related with land cover and building intensity
2 (Offerle et al., 2006).

3 China, with the largest population in the world, is one of the fastest growing and urbanizing
4 economies. So LULCC has an significant influence on the regional to global climate change
5 by altering the land surface energy and water flux in China (Zhao and Pitman, 2005; Suh and
6 Lee, 2004; Chen et al., 2014). Most field sites are built in the arid and semi-arid region. In the
7 northeastern ecotone between agriculture and animal husbandry, farmland has a greater
8 roughness and energy fluxes than grassland in Tongyu (Feng et al., 2012) but less than reed
9 wetland in Panjin (Li et al., 2009). In the degraded grassland in West China, the oasis-desert
10 transition zone is a cold source relative to the Gobi in Dunhuang (Wang et al., 2005), and
11 energy fluxes are different over different land surface due to vegetation, precipitation and soil
12 moisture in Loess Plateau (Wang et al., 2010). Besides, rapid urban expansion has changed
13 heat fluxes in the Pearl River delta a lot (Lin et al., 2009) and has increased sensible heat flux
14 in Beijing (Zhang et al., 2009). There are obvious differences between different surface types,
15 including air temperature, soil moisture and surface radiation and energy budget (Zhao et al.,
16 2013; Zhang et al., 2014). In monsoon region, it is worth noting that land cover change both
17 in Tibet Plateau and Inner Mongolian from vegetated to bare land not only changed the local
18 surface heat and water flux, but also weakened East Asia summer monsoon circulation and
19 precipitation (Xue 1996; Li and Xue 2010) . Even though the changes in surface heat fluxes
20 can influence monsoon onset or weakening and precipitation (Hsu and Liu, 2003; Fu and
21 Yuan, 2001; Qiu, 2013; Xue et al., 2004) ,the study based on field observations are very
22 limited in the East Asian monsoon region (Bi et al., 2007) ,especially over the mid- to lower
23 reaches of Yangtze River Valley.

24 The mid- to lower reaches of Yangtze River Valley is located in the typical East Asian
25 monsoon region, where the land use and land cover has been experiencing rapid changes with
26 more complicated land use types due to the rapid urbanization, industrialization, and
27 development of agriculture and animal husbandry. Interaction between human activities and
28 monsoon climate is most intensive in this region. Under the background of monsoon climate,
29 studies about the differences in the diurnal and seasonal variations of the land-atmosphere
30 interaction over various surface types are almost blank in this region.

31 In order to better understand the characteristics and mechanisms for the exchanges of mass,
32 energy, and water vapor between the land surface and atmosphere in the mid- to lower

1 reaches of Yangtze River Valley, in the present study we analyze observations collected at
2 several ground sites over different surface types around Nanjing. These sites include a school
3 site in the urban area (hereafter [DX-urban](#)), the Xianling site in suburban Nanjing ([XL-](#)
4 [suburb](#)), a grassland site (LS-grass) and a farmland site (LS-crop) in Lishui County, which is
5 located in the countryside. Data used in this study were collected at these sites in the spring
6 and summer of 2013. The goals of the study are (1) to compare the seasonal and diurnal
7 variation of micro-meteorological elements over different land surface type, (2) to reveal the
8 differences in surface radiation budget, energy distribution between various surface types; and
9 (3) to calculate important surface parameters over different surface and investigate the
10 feedback of different surface types to the atmosphere and its impact on local climate. The
11 mechanisms for the surface-atmosphere feedback will be further investigated. This study will
12 fill the gap of observation scarcity in land-atmosphere interaction in the mid- to lower reaches
13 of Yangtze River Valley, and provide scientific evidences for the regional climate simulation
14 and climate change prediction.

15

16 **2 Data and methodology**

17 **2.1 Introduction of field sites**

18 The observations used in this study were collected at four field sites located in urban,
19 suburban, and countryside areas of Nanjing. The four sites are referred to as [DX-urban](#), [XL-](#)
20 [suburb](#), LS-grass and LS-crop hereafter.

21 The [DX-urban](#) site (Fig. 1a) is located at Baixia District of Nanjing ($32^{\circ}2'24''\text{N}$,
22 $118^{\circ}47'24''\text{E}$), which is the central urban area of Nanjing. Residential and commercial
23 buildings are dominant within the 500m radius centered around the [DX-urban](#) site, and
24 thereby the land surface type is a typical urban surface at this site. Average height of
25 buildings is 19.7m, and the building coverage is up to 70%.

26 The [XL-suburb](#) Site (Fig. 1b) is the key station in the experiment of Station for Observing
27 Regional Processes of the Earth System, Nanjing University (SORPES-NJU). It is located at
28 ($32^{\circ}7'143''\text{N}$, $118^{\circ}57'910''\text{E}$, 43m above sea level) in the eastern suburb of Nanjing, an
29 upwind area along the prevailing wind direction in Nanjing ([Ding et al., 2013](#)). The distance
30 between the [XL-suburb](#) Site and [DX-urban](#) Site is 18km. Within the 50m×50m area at the
31 [XL-suburb](#) site, the grass height is 7cm. Outside the site area are woodlands from

1 afforestation with a height of around 3m. This site is located inside the Xianling campus of
2 Nanjing University. Since its operation in 2011, continuous observations are measured
3 through a suite of equipment instruments. The observations include conventional
4 meteorological measurements at various levels, surface energy budget measurements,
5 boundary layer meteorological elements measurements, surface radiation measurements,
6 atmosphere components and aerosols measurements, etc. The data used in this study are
7 standard measurements at half-hour intervals.

8 The site (31°43'08"N, 118°58'51"E) at Lishui county is taken as a satellite site of the
9 SORPES-NJU. The distance between Lishui site and [DX-urban](#) site is 38km. Lishui site
10 consists of a pair of observational sites, one over the grassland (LS-grass, Fig. 1c) and the
11 other (LS-crop, Fig. 1d) over the farmland nearby. The grass height is about 60cm at the LS-
12 grass, and the observation period is from January 2012 to February 2014. Rice grows at LS-
13 crop in the summer (mid June to early November) and winter wheat grows in the winter (from
14 mid- to late November to early June of next year). [A series of agricultural activities occurred
15 in the cropland, including winter wheat harvest in late May, straw burning and rice irrigation
16 in early June.](#) The maximum height of wheat is 75cm. The observation period at LS-crop is
17 from January 2013 to February 2014. The distance between the two sites at Lishui is 1.62km.

18 **2.2 Micro-meteorological measurements**

19 The instruments used at the [XL-suburb](#) site include automatic weather station, eddy
20 covariance system (EC), energy balance system, and soil temperature / humidity observation
21 system. Table 1 lists the major measured variables, ranges, observation heights, and
22 instrument models. The same measurement method is applied at the [XL-suburb](#), LS-grass and
23 LS-crop sites. In the [DX-urban](#) site, there is no measurement of soil moisture and soil
24 temperature. The instrument of eddy-covariance and energy balance system are installed at
25 the top of 36.5m high tower on the roof of the building which is 22m high. The air
26 temperature and humidity can be observed by the tower-mounted system 9m high above the
27 roof.

28 The auto weather station (AG1000, Campbell) measures micro-meteorological elements of
29 temperature, pressure, relative humidity, wind speed and direction, precipitation, and surface
30 radiation components of upward/downward shortwave and longwave radiation fluxes. Ts is
31 measured by infrared detection sensor (IRTS-P, Apogee).

1 Momentum, sensible and latent heat fluxes are measured by the eddy covariance system
2 (EC3000, Campbell), which includes a three-dimensional sonic anemometer (CSAT-3) and a
3 infrared analyzer (LI7500) at 3m height. The sampling frequency is 10Hz for measurements
4 by the Data acquisition (CR5000). Strict correction and quality control ([Foken et al.,
5 2004](#)) have been performed for all the turbulence measurements. Coordinate rotation
6 correction (Wilczak et al., 2001), frequency response correction (Moore, 1986), and WPL
7 correction etc. are applied in this study.

8 The soil heat flux plate (HFP01SC-L, Hukseflux) is at the depth of 8cm. At LS-grass and LS-
9 crop sites, the soil heat flux is measured at 5cm and 10cm below the ground, respectively.
10 Soil temperature and moisture at 5cm, 10cm, 20cm, 40cm, and 80cm are measured using Soil
11 Temperature Profile Sensor (STP01-L, Hukseflux) and Water Content Analyzer (S616-L,
12 Cambell). No soil temperature and moisture measurements are conducted at the [DX-urban](#)
13 site.

14 The data collected at the spring and summer (from March to August) of 2013 are used in the
15 present study. This is because the measurements are relatively complete during this period,
16 which is also the time when land-atmosphere interaction is strong.

17 **2.3 Methodology**

18 **2.3.1 Distribution of surface energy**

19 In the surface with fractional vegetation cover, surface energy budget can be expressed as

$$20 \quad R_n = H + L_E + G_0 + R_e$$

21 (1)

22 Where R_n is the net radiation which can be calculated by $R_n = DSR + DLR - USR - ULR$.
23 Four radiation components in this equation are respectively downward shortwave
24 radiation(DSR), downward longwave radiation(DLR), upward shortwave radiation(USR) and
25 upward longwave radiation(ULR). ~~Where R_n is the net radiation,~~ H and LE are the sensible
26 and latent heat fluxes respectively, G_0 is the soil heat flux at the surface, R_e is the remaining
27 term, which is associated with the photosynthesis and respiration of plants as well as
28 vegetation and soil thermal storage, etc. (Burba et al., 1999; Harazono et al., 1998). While in
29 the urban areas, the energy balance must take anthropogenic and net storage heat flux but not

1 G_0 into consideration (Oke, 1987). In this paper, we only discuss the relationship between H,
2 LE and R_n on the basis of the observation.

3 R_n can be calculated from the four radiation components. Sensible and latent heat fluxes are
4 calculated by the following equations:

$$5 \quad H = \overline{\rho c_p w' T'}$$

6 (2)

$$7 \quad L_E = \overline{\rho L_v w' q'}$$

8 (3)

9 where ρ , C_p and L are the air density (kg m^{-3}), the specific heat capacity at constant
10 pressure ($\text{J kg}^{-1} \text{K}^{-1}$), and latent heat of vaporization (J kg^{-1}). w' , T' and q' are
11 perturbations of vertical velocity (m/s), temperature (K), and mixing ratio of water vapor
12 (g/kg), respectively. Strict quality control has been conducted for all the flux measurements.

13 **2.3.2 Parameters related to the land surface process**

14 Surface albedo can be calculated based on the equation below (Zhang et al., 2004):

$$15 \quad \alpha = \frac{\sum \text{USR}}{\sum \text{DSR}}$$

16 (4)

17 where ~~both USR and DSR are~~ R_{sr} is the surface reflected radiation at half-hour interval, R_{sd} is
18 ~~the solar radiation that reaches the surface~~. This method to a certain degree can avoid the
19 adverse influence of low albedo on the calculation of daily average solar radiation when the
20 solar zenith angle is too low. Daily average albedo is the ratio between the upward and
21 downward solar radiation at half-hour interval during the period from 6:00 to 18:00 LST.

22 Following the same approach used in Li (2015), Bowen ratio is calculated based on the ratio
23 of H and LE. It is expressed as:

$$24 \quad \beta = \frac{\sum H}{\sum LE}$$

25 (5)

1 H and L_E are sensible and latent heat fluxes at half-hour interval, respectively. Daily Bowen
2 ratio is the ratio between the sum of sensible and latent heat fluxes at half-hour interval over
3 the entire day. The ratio between sensible and latent heat fluxes at the same time is taken as
4 the Bowen ratio at that same time.

5 Following the independent method proposed by Chen (1993), which determines z_{0m} using
6 only the mean wind speed and turbulence measured by ultrasonic anemometer, we fit the non-
7 dimensional wind speed ku / u^* to the stability parameter z / L in a double logarithmic
8 coordinate and obtain the value of ku/u^* under neutral condition. It is then applied to wind
9 profile equation under neutral condition and yields:

$$10 \quad z_{0m} = (z - d)e^{-\frac{ku}{u^*}}$$

11 (6)

12 where u is the horizontal wind speed (m/s); k is the Von Karman constant, which is set to be
13 0.4 in this study (Prueger et al., 2004); z is the height of the instrument probe (m); d is the zero
14 displacement, which is 2m at [XL-suburb](#) site, 0.4m at LS-grass site and 0.5m at LS-crop site.
15 u^* is the friction velocity ($m s^{-1}$); z_{0m} is the aerodynamic roughness length. Liu (2015)
16 verified this independent method using measurements from the semi-arid region in China.

17

18 **3 Results and discussion**

19 **3.1 Differences in micro-meteorological elements**

20 The year [of 2013 is an extremely drought period in southern](#)~~a typical hot and dry year in~~
21 [China, the precipitation decreased by more than 78% of the average amount in summer,](#)
22 [breaking the historical record over the past 50 years \(Yuan et al., 2016\)](#), especially in the mid-
23 to lower reaches of Yangtze River Valley (Han and He, 2014). Fig. 2 shows the daily
24 variations of air temperature, surface temperature, and relative humidity at the four field sites.
25 Surface temperature is calculated based on measured upward and downward longwave
26 radiation and the Stefan-Boltzmann law. Realistic daily changing trends of temperature and
27 humidity are displayed for the four sites, and maximum values of air temperature and surface
28 temperature both occur in August. The changing trend of relative humidity is similar to that of
29 precipitation, and the relative humidity tends to reach saturate at stations where there is more
30 precipitation and higher temperature. Fig.2 shows clearly that large differences in temperature

1 and humidity between the four sites mainly appear at April and August, when precipitation is
2 relatively small. The largest air temperature difference of 3.21°C is found between DX-urban
3 and LS-crop sites at the beginning of August, and the largest surface temperature difference is
4 7.26°C. The largest relative humidity difference is 22.79%. Apparently, even in the same
5 climate background, there exist significant differences in micro-meteorological elements
6 between various surface types. Such differences are more distinct when there is no
7 precipitation or precipitation is relatively small. Generally, surface temperature increases
8 when vegetation cover fraction decreases except in the farmland, which is affected by
9 irrigation. This is consistent with findings from some experiments in mid-latitudes of North
10 America (Lee X. et al., 2011; Li et al., 2015). Table 2 clearly indicates that, except that the
11 minimum summer temperature is found at XL-suburb site, extremely high/low values of
12 seasonal average air temperature, surface temperature, and relative humidity all occur at either
13 LS-crop site or DX-urban site, which are the two sites that are most affected by human
14 activities.

15 Fig. 3a and 3b suggest that the diurnal variations of both air temperature and surface
16 temperature exhibit single-peak feature in the spring and summer. The minimum value occurs
17 at 7:00 LST in the morning and the maximum value occurs in the afternoon. The variation of
18 air temperature lags that of surface temperature. The peak time of both air and surface
19 temperature in spring lags that in summer. ~~The air temperature variation lags that of the~~
20 ~~surface temperature, and it also lags in the summer that in the spring. Due to the influence of~~
21 ~~the surface, diurnal surface temperature range is larger than the diurnal range of air~~
22 ~~temperature.~~ Except for the LS-crop site, surface temperature is higher than air temperature in
23 all the other three sites. Nighttime air temperature and surface temperature at the DX-urban
24 site is higher than that in other sites by nearly 2°C due to the urban heat island effects. But
25 UHI is not typical in daytime, the extreme drought weakens this UHI and even makes the
26 peak temperature at suburb site and grass site higher than urban site. Natural drought may not
27 have a large effect at urban site or crop site because of human activities like watering or
28 irrigation, but at grass site and suburb site, the evaporation cooling is decrease distinctly.
29 Comparing the land surfaces that have vegetation cover, the grass height is low at the XL-
30 suburb site and the peak surface temperature variation is large with the largest temperature up
31 to 37.61°C. The peak surface temperature remains low at the LS-crop site due to irrigation,
32 and even lower than the daily maximum air temperature in the summer. The peak surface
33 temperature at the LS-crop site is only 32.4°C.

1 Due to the difference of radiation budget on land surface between daytime and nighttime,
2 diurnal surface temperature range is larger than the diurnal range of air temperature.

3 Comparing the diurnal temperature ranges at the four sites, it is found that the diurnal air
4 temperature and surface temperature ranges are 4.79°C and 9.26°C in the spring, respectively,
5 which are relatively small. In the summer, the LS-crop site is covered by water due to
6 irrigation and the diurnal surface temperature range is only 7.77°C, which is the minimum
7 among all the four sites. The diurnal air temperature range is 6.86°C at LS-grass site in the
8 summer, and the range is relatively large among all the sites. Meanwhile, the diurnal surface
9 temperature range at XL-suburb site is 12.46°C in the summer, the largest among the four
10 sites. Despite the large diurnal surface temperature range at XL-suburb site, air temperature
11 and diurnal air temperature range are not that large. This is because the afforest woodlands
12 surrounding the XL-suburb site promotes the heat flux exchange between the surface and
13 atmosphere.

14 Fig. 3c shows that the relative humidity is always larger in the summer than in the spring.
15 Daily maximum relative humidity occurs at around 7:00 am in the morning, and the minimum
16 value occurs at 16:00 in the afternoon. The occurrence of the maximum and minimum values
17 in the spring lags that in the summer. The maximum value is found at LS-crop, with the
18 summer average maximum value of 90.34%. The smallest relative humidity is found at the
19 DX-urban site, where the maximum summer average humidity is only 58.72%. The diurnal
20 relative humidity range at the four sites is larger in the spring than in the summer, and the
21 largest value is found at LS-crop site in the spring and at LS-grass in the summer with the
22 value of 39.03% and 27.36% respectively. The diurnal relative humidity range is the smallest
23 at the DX-urban site, which is 23.29% in the spring and 20.40% in the summer. Fig. 3 clearly
24 indicates that different surface types can lead to differences in surface temperature and impose
25 significant impacts on micro-meteorological elements such as air temperature and relative
26 humidity (Krishnan et al., 2012; Luyssaert et al., 2014).

27 **3.2 Surface net radiation and energy distribution**

28 **3.2.1 Distribution of net radiation**

29 Fig. 4 displays the daily variation of the four components of surface radiation flux, ~~i.e. the~~
30 ~~downward shortwave radiation (DSR), upward shortwave radiation (USR), downward~~
31 ~~longwave radiation (DLR), and upward longwave radiation (ULR).~~ DSR ~~is and USR are~~
32 mainly affected by clouds and aerosols in the atmosphere. In the monsoon region of the mid-

1 to lower reaches of Yangtze River Valley, the cloudy and rainy weather is dominant during
2 the period of May to July, leading to lower shortwave radiation despite the higher solar zenith
3 angle. Under the same climate background, DSR and DLR are similar at the four sites.
4 However, large differences are found in USR and ULR at the four sites. This is because USR
5 is related to surface albedo while ULR is associated with surface temperature. Daily
6 maximum values of USR and ULR both occur in early August. The maximum value of USR
7 are 48.67、55.29、35.80 and 52.19Wm⁻² at the LS-grass, LS-crop, DX-urban, and XL-suburb
8 sites respectively. The maximum value of ULR at the sour sites are 515.22、492.78、529.59
9 and 518.81W m⁻² respectively.

10 USR changes following the changes in DSR and surface albedo. Variability of monthly
11 average USR (Fig.5b) is similar to that of DSR (Fig. 5a), and both are the smallest at the DX-
12 urban site. However, compared to that in other sites, the USR at the LS-crop decreases rapidly
13 since May and reaches its minimum of 14.87 Wm⁻² at the end of June. This is because of the
14 albedo decrease at the LS-crop site, which is caused by straw burning at the end of May after
15 the winter wheat harvest. Rice starts growing since late June, and the USR at LS-crop site
16 becomes similar to that at other sites by August. The ULR remains largest at the DX-urban
17 site and smallest at LS-crop site, which is attributed to the increases in vegetation cover
18 fraction from May to August and irrigation at the LS-crop site. The difference in ULR
19 between the DX-urban and LS-crop can be up to 26.9 W m⁻² in August.

20 With the same weather and climate background, there are no significant differences in DSR
21 and DLR among the four sites, despite their distinct seasonal differences. The maximum daily
22 DSR are around 550 W m⁻² and 600W m⁻² in the spring and summer respectively, and the
23 maximum daily DLR are about 370 W m⁻² and 450 W m⁻² in the spring and summer
24 respectively. Fig. 6c shows that the maximum daily average USR at XL-suburb, LS-grass and
25 DX-urban grows to 90.35、84.79、59.49 W m⁻² in the summer. Unlike these three sites, USR
26 at crop site at decreases the LS crop site is smaller in the summer than in the spring by 16.98
27 Wm⁻² form spring to summer due to the continuous lower albedo from June to early
28 July which is different from the situation in the other three sites, where surface albedo
29 increases in the summer due to the decreased vegetation cover fraction. As a result, the USR
30 decreases by 90.35、84.79、59.49 W m⁻² at LS crop, XL suburb, and DX urban sites
31 respectively. The diurnal variation of ULR (Fig. 6d) depends on diurnal variation of surface
32 temperature (Fig.2b). The largest ULR occurs at XL-suburb site in the daytime and at DX-

1 [urban](#) site in the nighttime. The maximum ULR and diurnal ULR range both are the smallest
2 at the LS-crop site due to irrigation.

3 **3.2.2 Surface energy distribution**

4 The land-atmosphere energy exchange is the driving force for the local climate and is under
5 great influence of climate change (Reale and Dirmeyer, 2000; Li et al., 2009). Fig. 7 shows
6 daily variation of net radiation (R_n), sensible heat flux (H), and latent heat flux (LE). R_n and
7 DSR have the similar changing trends and both are small during the monsoon precipitation
8 period. The average R_n during the growing season is different over different surface types,
9 and the values are 126.55, 118.40, 112.58, 105.08 $W m^{-2}$ at the LS-crop, LS-grass, [XL-suburb](#),
10 and [DX-urban](#) sites respectively. The average value of H during the growing season are 4.62,
11 39.99, 26.13, 53.48 $W m^{-2}$ respectively at the four sites, while LE are 74.11, 53.59, 59.73, and
12 34.45 $W m^{-2}$ respectively. The above results suggest that under the same large scale forcing,
13 there exist distinct differences in radiation and turbulent fluxes over different surface types.
14 Such kinds of differences are the largest between LS-crop and [DX-urban](#) sites, where human
15 activities are the most intensive among the four sites. During the non-precipitation period,
16 differences in R_n and H are large in July and August, with absolute value of differences up to
17 79.88 and 166.56 $W m^{-2}$ respectively. At the beginning of April, with little precipitation and
18 insufficient soil moisture content, irrigation at the LS-crop site leads to the LE difference to
19 be up to 107.87 $W m^{-2}$. The above differences are largely caused by the difference in
20 vegetation cover at the surface and associated with the growth of vegetation and accompanied
21 water cost.

22 Monthly average R_n reaches the largest in July and the value at LS-crop is 170.37 $W m^{-2}$.
23 Since the rainy season starts, the proportion of LE in R_n gradually increases. Although the
24 monthly variation of R_n are similar at the four sites (Fig. 8a), there exist large differences in
25 sensible and latent heat flux (Fig. 8b, 8c). H is smallest at the LS-crop. Rice planting starts in
26 mid June and the surface is covered by water. Negative sensible heat flux occurs in July and
27 August at the LS-crop site. The difference in sensible heat flux between the LS-crop and [DX-](#)
28 [urban](#) sites is 44.86 $W m^{-2}$. The change of LE is opposite to that of H. LE reaches the largest in
29 July and August with the value greater than 95 $W m^{-2}$. LE is 55.68 $W m^{-2}$ larger at the LS-site
30 than at the [DX-urban](#) site.

31 Fig. 9 depicts the seasonal average surface energy components. H accounts for a large
32 proportion of R_n in the spring, with the value ascending from 25.60%, 47.65%, 60.92% to

1 75.45% at LS-crop, LS-grass, [XL-suburb](#), and [DX-urban](#) sites. In the summer, accompanied
2 with the rainy season, vegetation thrives and the ratio of LE/R_n significantly increases. The
3 values are 60.01%, 47.18%, 66.65% and 37.86% respectively at the four sites. Again effects
4 of the woodlands surrounding the [XL-suburb](#) site are reflected in the measurements at [XL-](#)
5 [suburb](#). The negative sensible heat flux is attributed to the negative difference in air
6 temperature and surface temperature (Table 1) at the LS-crop site.

7 Fig. 10 shows the diurnal variations of net radiation, sensible heat flux, and latent heat flux
8 for the spring and summer at the four sites. R_n is negative at the nighttime and the maximum
9 value occurs at around 14:00 in the daytime. The differences in peak value of R_n between the
10 spring and summer are larger than 50 W m^{-2} at all the four sites. Except for the [DX-urban](#) site,
11 the difference in maximum H between the spring and summer is greater than 30 W m^{-2} at the
12 other three sites. The difference in the peak value of LE between the spring and summer is
13 larger than 60 W m^{-2} . At the [DX-urban](#) site, H is always larger than LE in both the spring and
14 summer. Fig. 10b shows clearly that the peak value of H is largest at the [XL-suburb](#) site in the
15 spring, and at [DX-urban](#) site in the summer. The differences between these two sites and the
16 LS-crop site are 92.53 and 162.21 W m^{-2} respectively. The peak value of H is the smallest at
17 the LS-crop site, and H can be negative during the entire day in the summer. This is because
18 the LS-crop site is covered by water in the summer, and the large evaporation results in low
19 surface temperature that is lower than air temperature (Lee et al., 2004). For both the spring
20 and summer, the peak value of LE remains largest at the LS-crop site and smallest at the [DX-](#)
21 [urban](#) site. The difference in LE between the two sites can be up to 138.46 W m^{-2} in the spring
22 and 156.46 W m^{-2} in the summer. This result suggests that there exist distinct differences in
23 radiation and surface energy fluxes over different underlying surface types not only in the
24 semiarid region (Wang et al, 2010; Li et al., 2015), but also in the monsoon region of mid- to
25 lower reaches of Yangtze River valley.

26 **3.3 Mechanism analysis**

27 Changes in the surface characteristics are always accompanied by variations in the parameters
28 involved in land surface process. Differences in characteristic parameters such as albedo,
29 Bowen ratio, roughness length, etc affect radiation and energy distribution, which
30 subsequently feedback to the atmosphere and affect micro-meteorology in the surface layer
31 (Amiro et al., 2006; Lee et al., 2011).

3.3.1 Radiation and turbulent exchange coefficients

In land surface processes, albedo is a basic parameter that affects net radiation in the surface (Li et al., 2015; Krishnan et al., 2012; Zhang et al., 2014). Daily variations of albedo at three ~~the four~~ sites with vegetation (Fig.11a) show that albedo decreases with the growing of vegetation from March to mid May, and keeps stable in June, then slightly increases until August because of lacking precipitation. The rapid decrease is found in the LS-crop site with the largest daily decrease of 0.13. At the beginning of June, albedo decreases to less than 0.09 due to the straw burning and later remains less than 0.1 due to irrigation. Since mid July, the albedo at the LS-crop site gradually increases to 0.15 accompanied with the growing of rice, and becomes close to that at DX-urban and XL-suburb sites. At DX-urban site, there is no large daily variation of albedo, which remains at around 0.13. Besides, there exists a high correlation between albedo and precipitation for DX-urban and LS-crop sites but not LS-grass or XL-suburb. The roof is watertight in the city and the soil with sparse vegetation cover has high soil wetness in cropland. After precipitation, the waterlogging both occurs at these two sites, which cause the high albedo in a short time.

The difference in albedo determines the daily USR variation at the four sites (Fig. 4b). Fig. 12 shows that except for XL-suburb site, the albedo at the other three sites decrease from spring to summer is smaller in the summer than in the spring, which is mainly related to the growing of vegetation. At the XL-suburb site, possibly because of insufficient precipitation after mid July, the summer albedo increases and becomes slightly larger than that in the spring. But at grassland, the albedo decreases largely in the green-up phrase, which results in the lower albedo in summer. And the dramatic decrease of surface albedo in early June is associated with the biomass burning due to the cultivation system in this region, i.e., a rotation of wheat in winter and rice in summer. Even with the influence of irrigation and albedo increase, however, If not considering irrigation in the LS-crop site, albedo always decreases with the increase of vegetation cover fraction, while the radiative forcing still leads to the increase of surface temperature increases in surface temperature. In the boreal region, however, model studies and field experiments both have revealed that (Defries et al., 2002; Lee et al., 2011) degradation of vegetation represented by deforestation could lead to lower surface temperature. This is quite different from the situation in temperate and tropical regions. Thereby, the warming and cooling trends might be different over regions with different

1 surface types and background climate, which makes it important to conduct mechanism study
2 for the impact of different land cover types on local temperature.

3 Bowen ratio is the measure of surface energy distribution. It reflects the dry and wet condition
4 of the surface to a certain degree (Li et al., 2015; Wang et al., 2010). The daily variation of
5 the Bowen ratio (Fig. 11b) indicates that large variation occurs in the spring and there exist
6 distinct differences between the four sites. The difference between the DX-urban and LS-crop
7 sites is larger than 10 at the beginning of March. The differences between the four sites and
8 the variation at each site both decrease during the rainy season. Except for the DX-urban site,
9 Bowen ratio is smaller than 1.0 since early May at all the other three sites and LE becomes
10 dominant. Considering the surface types at the four sites, it is found that daily variation of
11 Bowen ratio is small (stable) at the surface with large vegetation cover fraction and high soil
12 moisture content, which is more capable of adjusting the heat and water balance. This result is
13 consistent to that for the semiarid region (Hu et al., 2009). Fig. 12b suggests that with more
14 precipitation and large vegetation cover fraction in the summer, the Bowen ratio is much
15 smaller in the summer than in the spring. Comparing the Bowen ratio at the four sites, the
16 largest value is found at the DX-urban site while the smallest is at the LS-crop site for both
17 the spring and summer. The negative sensible heat flux at the LS-crop site in the summer
18 makes the Bowen ratio to be less than zero. At the XL-suburb site, H/LE further decreases
19 due to the effects of woodlands nearby, while LE/R_n further increases and accounts for a
20 larger proportion in the energy distribution (Fig. 9b).

21 Generally speaking, LE accounts for a large proportion of R_n at sites where Bowen ratio is
22 small. ~~Since the relative humidity is affected by temperature and water vapor content, it will~~
23 ~~increase with the decrease in Bowen ratio and temperature (Li et al., 2015), which~~ This
24 ~~relation~~ is basically ~~shown~~satisfied in the mid- to lower reaches of Yangtze River Valley, ~~but~~
25 ~~relative humidity can not be entirely analyzed without considering the influence of~~
26 ~~advection because of data limitation. but the general situation becomes more complicated due~~
27 ~~to the influences of many other factors.~~

28

29 **3.3.2 Surface roughness length at different surface types**

30 Surface roughness length is an important ecological and land surface parameter. The spring-
31 summer average roughness length at the DX-urban site calculated based on the shape of the

1 surface roughness elements is 2.82m, which has no distinct seasonal variation. Monthly
2 variations of surface roughness length at the other three sites are shown in Fig. 13, which
3 shows that the roughness length basically increases with the month from May to August. The
4 differences in roughness length between the four sites are largely caused by the differences in
5 vegetation cover, which are rice, grass, and lawn at the LS-crop, LS-grass, and XL-suburb
6 sites. The average roughness lengths ~~ofat the three sites during~~ the growing season are
7 0.020-0.05m, 0.050-0.02m, and 0.17m respectively at these three sites. Apparently the roughness
8 length at the XL-suburb site more reflects the characteristics of the woodlands nearby. The
9 roughness length decreases slightly in July at XL-suburb and LS-grass sites due to insufficient
10 precipitation. In early June after the harvest of winter wheat, the roughness length at the LS-
11 crop is less than 0.01m, but it gradually increases later with the growth of rice.

12 Fig. 14 shows that from the spring to summer, the increase in roughness length at the XL-
13 suburb site is much larger than that at the LS-grass site, and the differences between the
14 spring and summer at the two sites are 0.045m and 0.007m respectively. This is attributed to
15 the differences in vegetation type and height. This result indicates that different land use type
16 and roughness element height are responsible for the different roughness length at various
17 time scales.

18 Comparing results at LS-grass and XL-suburb sites, both are covered by natural vegetation, it
19 can be found that the vegetation with larger roughness length can promote stronger turbulent
20 flux transfer and has a higher capability of temperature adjustment. This explains why
21 average temperature and diurnal temperature range both are relatively small at XL-suburb site,
22 despite the high surface temperature at this site (Fig. 3a). Sensitivity experiments of a
23 numerical model study also demonstrated that the surface roughness length is one of the most
24 sensitive factors for land-atmosphere exchange (Liu et al., 2015).

25

26 **4 Conclusions and discussion**

27 2013 is a typical dry and hot year. During the growing season in the mid- to lower reaches of
28 Yangtze River Valley monsoon region, the four different surface types, i.e. urban surface,
29 woodland, grassland, and cropland, can directly affect the surface radiation balance and land-
30 atmosphere exchanges of heat, water vapor, and mass fluxes, and subsequently affect local
31 climate. In the present study, we have revealed the differences in several physical parameters

1 between the four typical surface types mentioned above during the study period and explored
2 the mechanisms for the differences.

3 Daily variations of the micro-meteorological elements at the four sites are different due to
4 different surface characteristics. The differences in micro-meteorological elements are more
5 distinct during the dry and hot period. The differences between the DX-urban and LS-crop
6 sites are the most significant. The largest differences in air temperature, surface temperature,
7 and relative humidity between the two sites are 3.21°C, 7.26°C, and 22.79% respectively.
8 Compared with ~~that over the land use type covered by~~ natural vegetation cover (LS-grass and
9 XL-suburb sites), albedo at urban surface is smaller and thus the radiative forcing is stronger,
10 leading to higher surface temperature. However, insufficient moisture content makes the
11 Bowen ratio large. Hence the surface heat is transferred to the atmosphere mainly in the form
12 of sensible heat flux, and air temperature is high while relative humidity is small. Meanwhile,
13 the urban heat island effect results in higher surface T_a and T_s in the nighttime at the DX-
14 urban site that is 2°C higher than at other sites, and the diurnal temperature range is small.
15 At Lishui county, the crops were not stressed by lack of moisture or high temperatures during
16 the growing period due to irrigation, so latent heat flux dominates the land-atmosphere heat
17 flux exchange. Surface temperature and air temperature both are relatively low while the
18 relative humidity is relatively large due to large evaporation at the surface. Surface albedo
19 reaches its smallest value in June because of wheat harvest and straw burning at this time.
20 Daily variation of USR increases under the influence of albedo. For both spring and summer,
21 the peak value of diurnal variation of surface temperature and diurnal temperature range are
22 the smallest at the DS-crop site, mainly because the sufficient soil moisture content at this site
23 acts to lower the surface temperature. Negative sensible heat flux is found at this site in the
24 summer due to the large evaporation. Compared with the situation over surface types with
25 natural vegetation cover, peak value in the diurnal variation of surface temperature and its
26 diurnal range both are large at the XL-suburb site, where vegetation cover fraction is low.
27 However, the woodland nearby the XL-suburb promotes turbulent exchange and heat flux
28 transfer, leading to lower air temperature and its diurnal range. From the spring to summer,
29 latent heat flux becomes dominant with the increase of albedo, and the Bowen ratio gradually
30 decreases to less than 1. Diurnal ranges of air temperature, surface temperature, and relative
31 humidity all gradually decrease.

1 Under the same climate background, changes in surface albedo result in changes in the
2 radiative forcing. The Bowen ratio change caused by the surface energy distribution and the
3 aerodynamic resistance change related to surface roughness length jointly determine the
4 differences in surface temperature, air temperature, and relative humidity between different
5 land surface types with various vegetation cover. The monsoon precipitation and land use
6 changes by human activities makes the land-atmosphere interaction more complicated.
7 Compared with the situation at sites with natural vegetation cover, air temperature at the [XL-](#)
8 [suburb](#) site is smaller than that at the LS-grass site, whereas the surface temperature is higher
9 than that at the LS-grass site. Such a inconsistency is caused by the complexity in the surface
10 characteristics. The present study has investigated the features and mechanisms of land-
11 atmosphere interaction over four different surface types. However, contributions of various
12 land surface parameters to micro-meteorological elements are different, and further
13 quantitative analysis of the contribution of each individual parameter is necessary.

14

15 **Acknowledgements**

16 This research is jointly sponsored by Natural Science Foundation of China (Grant No.
17 41475063, 91544231), the National Science and Technology Support Program
18 (2014BAC22B04), and Program for New Century Excellent Talents in University. This work
19 is also supported by the Jiangsu Collaborative Innovation Center for Climate Change.

1 **References**

- 2 Amiro, B. D., Barr, A. G., Black, T.A., Iwashita, H., Kljun, N., McCaughey, J. H., Mor-
3 genstern, K., Murayama, S., Nesic, Z., Orchansky, A. L., Saigusa, N.: Carbon, energy and
4 water fluxes at mature and disturbed forest sites, Saskatchewan, Canada, *Agr. Forest.*
5 *Meteorol.*, 136, 237–251, 2006.
- 6 Alberto M.C.R., Wassmann R., Hirano T., Miyata A., Hatano R., Kumar A., Padre A.,
7 Amante M.: Comparisons of energy balance and evapotranspiration between flooded and
8 aerobic rice fields in the Philippines, *Agric Water Manag*, 98, 1417–1430, 2011.
- 9 Alberto, M.C.R., Wassmann, R., Hirano, T., Miyata, A., Arvind, K., Padre, A., Amante, M.:
10 CO₂/heat fluxes in rice fields: Comparative assessment of flooded and non-flooded fields in
11 the Philippines, *Agric. Forest Meteorol.* 149, 1737–1750, 2009.
- 12 Arnfield, A. J.: Two decades of urban climate research: A review of turbulence, exchanges of
13 energy and water, and the urban heat island, *Int. J. Climatol.*, 23, 1–26, doi:10.1002/joc.859,
14 2003.
- 15 Baldocchi D. D.: Biogeochemistry: Managing land and climate, *Nature Climate Change*, 4,
16 330-331, 2014.
- 17 Baldocchi, D. D., and Ma, S.: How will land use affect air temperature in the surface
18 boundary layer? Lessons learned from a comparative study on the energy balance of an oak
19 savanna and annual grassland in California, USA, *Tellus B*, 65, 1999, 2013,
20 <http://dx.doi.org/10.3402/tellusb.v65i0.19994>.
- 21 Baldocchi, D. D., Xu, L., Kiang N.: How plant functional-type, weather, seasonal drought,
22 and soil physical properties alter water and energy fluxes of an oak–grass savanna and an
23 annual grassland, *Agr. Forest. Meteorol.*, 123, 13-39, 2004.
- 24 Baldocchi, D. D., and Coauthors: FLUXNET: A new tool to study the temporal and spatial
25 variability of ecosystem–scale carbon dioxide, water vapor, and energy flux densities, *Bull.*
26 *Amer. Meteor. Soc.*, 82, 2415–2434, 2001.
- 27 Baldocchi, D. D., and Rao, K. S.: Intra-field variability of scalar flux densities across a
28 transition between a desert and an irrigated potato field, *Boundary-Layer Meteorology*, 76,
29 109-136, 1995.

- 1 Bi, X., Gao, Z., Deng, X., Wu, D., Liang, J., Zhang, H., Sparrow, M., Du, J., Li, F., and Tan,
2 H.: Seasonal and diurnal variations in moisture, heat, and CO₂ fluxes over grassland in the
3 tropical monsoon region of southern China, *J. Geophys. Res.*, 112, D10106,2007.
- 4 Bonan, G. B.: Forests and climate change: forcings, feedbacks, and the climate benefits from
5 the forests, *Science* 320, 1444–1449, 2008.
- 6 Bounoua, L., DeFries, R., Collatz, G. J., Sellers, P., Khan, H.: Effects of land cover
7 conversion on surface climate, *Clim. Change*, 52,29,2002.
- 8 Brown, M., Black, T. A., Nesic, Z., et al.: Impact of mountain pine beetle on the net
9 ecosystem production of lodgepole pine stands in British Columbia, *Agr. Forest. Meteorol.*,
10 150: 254–264,2010.
- 11 Burba, G. G., Verma, S. B., and Kim, J.: Surface energy fluxes of *Phragmites australis* in a
12 prairie wetland, *Agr. Forest. Meteorol.*, 94,31–51,1999.
- 13 Chen, J., Wang, J, and Mitsuta, Y.: An independent method to determine the surface
14 roughness length (in Chinese), *Chinese J. Atmos. Sci.*, 17, 21–26, 1993.
- 15 Chen, X., Su, Z., Ma, Y., Liu, S., Yu, Q. , Xu, Z.: Development of a 10-year (2001–2010)
16 0.1° data set of land-surface energy balance for mainland China, *Atmos. Chem. Phys.*, 14:
17 13097-13117, 2014.
- 18 Coulter, R. L., Pekour, M. S., and Cook. D. R.: Surface energy and carbon dioxide fluxes
19 above different vegetation types within ABLE, *Agr. Forest. Meteorol.*, 136, 147–158, 2006.
- 20 Davin, E. L., and De Noblet-Ducoudré, N.: Climatic impact of global-scale deforestation:
21 radiative versus nonradiative processes, *J. Clim.* 23, 97–112, 2010.
- 22 Defries, R. S., Bounoua, L., Collatz, G. J.: Human modification of the landscape and surface
23 climate in the next fifty years, *Global Change Biology*, 8:438-458, 2002.
- 24 [Ding A J, Fu C B, Yang X Q, et al.: Intense atmospheric pollution modifies weather: a case of](#)
25 [mixed biomass burning with fossil fuel combustion pollution in eastern China. *Atmospheric*](#)
26 [Chemistry & Physics, 13\(20\):10545-10554, 2013.](#)
- 27 Feddema, J. J., Oleson, K. W., Bonan, G., Mearns, L. O., Buja, L. E., Meehl, G. A.,
28 Washington, W. M.: The importance of land-cover change in simulating future climates,
29 *Science*, 310 , 1674–1678, 2005.

- 1 Feng, J. W., Liu, H. Z., Wang, L.: Seasonal and inter-annual variation of surface roughness
2 length and bulk transfer coefficients in semiarid area, *Sci. China Earth Sci.*, 55, 254–261, 2012.
- 3 [Foken T, Göckede M, Mauder M, et al. Post-Field Data Quality Control\[M\]// Handbook of
4 micrometeorology: a guide for surface flux measurement and analysis. , 2004:181-208.](#)
- 5 Fu, C. B., Yuan, H. L.: An virtual numerical experiment to understand the impacts of
6 recovering natural vegetation on the summer climate and environmental conditions in East
7 Asia, *Chinese Sci. Bull.* 46, 1199, 2001.
- 8 Gao, X. J., Luo, Y., Lin, W. T., Zhao, Z. C., Giorgi, F.: Simulation of effects of land use
9 change on climate in China by a regional climate model, *Adv. Atmos. Sci.* 20, 583, 2003.
- 10 Harazono, Y., Kim, J., Miyata, A., Choi, T., Yun, J.I., and Kim, J.W.: Measurement of energy
11 budget components during the International Rice Experiment (IREX) in Japan, *Hydrol.
12 Processes*, 12, 2081–2092, 1998.
- 13 Hu, Z., Yu, G., Zhou, Y., et al.: Partitioning of evapotranspiration and its controls in four
14 grassland ecosystems: application of a two-source model, *Agr. Forest. Meteorol.*, 149:1410–
15 1420, 2009.
- 16 Hsu, H.-H., and Liu, X.: Relationship between the Tibetan Plateau heating and East Asian
17 summer monsoon rainfall, *Geophys. Res. Lett.*, 30, 2066, doi:10.1029/2003gl017909, 2003.
- 18 Intergovernmental Panel on Climate Change: *Climate Change 2013: The Physical Science
19 Basis. Contribution of Working Group I to the Fifth Assessment Report of the
20 Intergovernmental Panel on Climate Change* [Stocker, T.F., D. Qin, G.-K. Plattner, M. Tignor,
21 S.K. Allen, J. Boschung, A. Nauels, Y. Xia, V. Bex and P.M. Midgley (eds.)]. Cambridge
22 University Press, Cambridge, United Kingdom and New York, NY, USA, 1535, 2013.
- 23 Jin, Y., Roy, P.D.: Fire-induced albedo change and its radiative forcing at the surface in
24 northern Australia, *Geophys. Res. Lett.* 32, L13401, 2005.
- 25 Kalnay, E., Cai, M.: Impact of urbanization and land-use change on climate, *Nature*, 423,
26 528–531, 2003.
- 27 Krishnan, P., Meyers, T. P., Scott, R. L., et al.: Energy exchange and evapotranspiration
28 over two temperate semi-arid grasslands in North America, *Agr. Forest. Meteorol.*, 153, 31-44,
29 2012.

- 1 Lawrence, P. J., Feddema, J. J., Bonan, G. B.: Simulating the biogeochemical and
2 biogeophysical impacts of transient land cover change and wood harvest in the Community
3 Climate System Model (CCSM4) from 1850 to 2100, *J. Clim.* 25, 3071–3095, 2012.
- 4 Lee, E., Barford, C., Kucharik, C., Felzer, B., and Foley, J.: Role of turbulent heat fluxes over
5 land in the monsoon over East Asia, *Int. J. Geosci.*, 2, 420–431, 10.4236/ijg.2011.24046.,
6 2011.
- 7 Lee, X., Goulden, M. L., Hollinger, D. Y.: Observed increase in local cooling effect of
8 deforestation at higher latitudes, *Nature*, 479, 384-387, 2011.
- 9 Lee, X., Qiang, Y., Sun, X., et al.: Micrometeorological fluxes under the influence of regional
10 and local advection: a revisit, *Agr. Forest. Meteorol.*, 122,111–124, 2004.
- 11 Li, Y. J., Zhou, L., Xu, Z. Z., and Zhou, G. S.: Comparison of water vapor, heat and energy
12 exchanges over agricultural and wetland ecosystems, *Hydrol. Processes*, 23, 2069–2080, 2009.
- 13 Li, H. Y., Fu, C. B., Guo, W. D., Ma, F.: Study of energy partitioning and its feedback on the
14 microclimate over different surfaces in an arid zone (in Chinese), *Acta Phys. Sin.*, 64, 059201,
15 2015.
- 16 Lin, W., Zhang, L., Du, D., Yang, L., Lin, H., Zhang, Y., and Li, J.: Quantification of land
17 use/land cover changes in Pearl River Delta and its impact on regional climate in summer
18 using numerical modeling, *Reg. Environ. Change*, 9, 75–82,doi:10.1007/s10113-008-0057-5,
19 2009.
- 20 Liu, Y., Guo, W. D., Song, Y. M.: Estimation of key surface parameters in semi-arid region
21 and their impacts on improvement of surface fluxes simulation, *Sci. China Earth Sci.* doi:
22 10.1007/s11430-015-5140-4, 2015.
- 23 Lohila, A., Minkinen, K., Laine, J.: Forestation of boreal peatlands: impacts of changing
24 albedo and greenhouse gas fluxes on radiative forcing, *J. Geophys. Res.* 115, G04011, 2010.
- 25 Luysaert, S. et al.: Land management and land-cover change have impacts of similar
26 magnitude on surface temperature, *Nature Clim. Change* 4, 389–393, 2014.
- 27 Masseroni, D., Facchi, A., Romani, M., Chiaradia, E. A., Gharsallah, O., and Gandolfi, C.:
28 Surface energy flux measurements in a flooded and an aerobic rice field using a single eddy-
29 covariance system, *Paddy and Water Environment*, 13, 405-424, 2014

1 Montes-Helu, M. C., Kolb, T., Dore, S., Sullivan, B., Hart, S. C., Koch, G., Hungate, B. A.:
2 Persistent effects of fire-induced vegetation change on energy partitioning and
3 evapotranspiration in ponderosa pine forests, *Agr. Forest. Meteorol.*, 149, 491-500, 2009.

4 Moore, C. J.: Frequency response corrections for eddy correlation systems, *Boundary Layer*
5 *Meteorol.*, 37, 17–35, doi:10.1007/BF00122754, 1986.

6 Mcalpine, C.A., Syktus, J., Ryan, J.G., Deo, R.C., Mckeen, G.M.: A continent under stress:
7 interactions, feedbacks and risks associated with impact of modified land cover on Australia's
8 climate, *Glob. Change Biol.*, 15, 2206, 2009.

9 Offerle, B., Grimmond, C., Fortuniak, K., and Pawlak, W.: Intraurban differences of surface
10 energy fluxes in a central european city, *Journal of Applied Meteorology & Climatology*, 45,
11 125-136, 2006.

12 Oke, T.R., Cleugh, H.A.: Urban heat storage derived as energy balance residuals,
13 *Boundary layer Meteorology*, 39, 233-245, 1987.

14 Pielke, R. A., Marland, G., Betts, R. A., Chase, T. N., Eastman, J. L., Niles, J. O., Niyogi, D.
15 D. S., Running, S. W.: The influence of land-use change and landscape dynamics on the
16 climate system: relevance to climate-change policy beyond the radiative effect of greenhouse
17 gases, *Philosophical Transactions A* 360, 1705, 2002.

18 Pitman, A. J., Noblet-Ducoudre, N., Cruz, F. T. et al.: Uncertainties in climate responses to
19 past land cover change: First results from the LUCID inter-comparison study, *Geophys. Res.*
20 *Lett.*, 36, L14814, 2009.

21 Prueger, J. H., Kustas, W. P., Hipps, L. E., Hatfield, J. L.: Aerodynamic parameters and
22 sensible heat flux estimates for a semi-arid ecosystem, *J Arid Environ.*, 57, 87-100, 2004.

23 Qiu, J.: Monsoon Melee, *Science*, 340, 1400–1401, doi:10.1126/science.340.6139.1400, 2013.

24 Reale, O., Dirmeyer, P.: Modeling the effects of vegetation on Mediterranean climate during
25 the Roman Classical Period. Part I: Climate history and model sensitivity, *Global & Planetary*
26 *Change*, 25, 163-184, 2000.

27 Sanderson, E. W., Jaiteh, M., Levy, M. A., Redford, K. H., Wannebo, A. V., Woolmer, G.:
28 The human footprint and the last of the wild, *Bioscience*, 52, 891–904, 2002.

1 Suh, M.-S. and Lee, D.-K.: Impacts of land use/cover changes on surface climate over east
2 Asia for extreme climate cases using RegCM2, *J. Geophys. Res.-Atmos.*, 109,
3 D02108,doi:10.1029/2003jd003681, 2004.

4 Wang, G.Y., Huang, J. P., Guo, W. D., Zuo, J. Q., Wang, J. M., Bi, J. R., Huang ,Z. W., and
5 Shi, J. S.: Observation analysis of land-atmosphere interactions over the Loess Plateau of
6 northwest China, *J. Geophys. Res.*, 115, D00K17, 2010.

7 Wang, Q., and Eleuterio, D.P.: A comparison of bulk aerodynamic methods for calculating
8 air-sea fluxes, paper presented at Ninth Conference on Mesoscale Processes, *Am. Meteorol.*
9 *Soc.*, Fort Lauderdale, Fla., 2001.

10 Wang, S., Zhang, Q., Wei, G. A.: Analyses on Characters of Surface Radiation and Energy at
11 Oasis-Desert Transition Zone in Dunhuang (in Chinese), *Plateau Meteorology*, 24, 556-562,
12 2005.

13 Wang, Y., Sang, Y. Y., Zhang L. F.: Circulation anomaly of summer high temperature and
14 drought in Zhejiang of 2013, *Journal of the Meteorological Sciences*, 35, 140-149, doi:
15 10.3969 /2014jms.0086, 2015.

16 Werth, D., Avissar, R.: The local and global effects of Amazon deforestation, *J. Geophys.*
17 *Res.*, 107, 8087, 2002.

18 Wilczak, J. M., Oncley, S. P., and Stage, S.A., Sonic anemometer tilt correction algorithms,
19 *Boundary Layer Meteorol.*, 99, 127–150, doi:10.1023/A:1018966204465, 2001.

20 Xue, Y., Juang, H.-M. H., Li, W., Prince, S., DeFries, R., Jiao, Y., and Vasic, R.: Role of land
21 surface processes in monsoon development: East Asia and West Africa, *J. Geophys. Res.*, 109,
22 2004.

23 [Yuan W, Cai W, Yang C, et al. Severe summer heatwave and drought strongly reduced](#)
24 [carbon uptake in Southern China \[J\]. *Scientific Reports*, 6\(25\):87–90, doi: 10.1038/srep18813,](#)
25 [2016.](#)

26 Han, X., He, L.: Analysis of Abnormal High Temperature Causes in the Summer of 2013,
27 *Climate Change Research Letters*, 03:78-84, 2014.

28 Zhang, C., Chen, F., Miao, S., Li, Q., Xia, X., and Xuan, C.: Impacts of urban expansion and
29 future green planting on summer precipitation in the Beijing metropolitan area, *J. Geophys.*
30 *Res.-Atmos.*,114, D02116, doi:10.1029/2008jd010328, 2009.

- 1 Zhang, M., Lee, X., Yu, G., et al.: Response of surface air temperature to small-scale land
2 clearing across latitudes, *Environmental Research Letters*, 9:206-222, 2014.
- 3 Zhang, Q., Huang, R.: Water vapor exchange between soil and atmosphere over a Gobi
4 surface near an oasis in the summer, *Journal of Applied Meteorology*, 43, 1917-1928, 2004.
- 5 Zhang, T. T., Wen, J., Wei, Z. G., Rogier, V., Li Z. C., Liu, R., Lv S. N., Chen H.: Land-
6 atmospheric water and energy cycle of winter wheat, Loess Plateau, China, *Int. J.Clim.*,34,
7 3044-3053, 2014.
- 8 Zhao, M., Pitman, A. J.: The relative impact of regional scale land cover change and
9 increasing CO₂ over China, *Adv. Atmos. Sci.* 22, 58–68, 2005.
- 10 Zhao, Q. F., Guo, W. D., Ling, X. L., Liu, Y., Wang, G. Y., Xie, J.: Analysis of
11 evapotranspiration and water budget for various land use in semi-arid areas of Tongyu, China
12 (in Chinese), *Climatic Environ. Res.* 18 415, 2013.
- 13

1 Table 1. Instruments, measurement ranges, measurement heights, and instrument models.

Parameter/Variable Name Description	Range	Measurement Height	Instrument
Wind speed sensor	0–45 m/s	2.0m	Met One, 014A-L
Humidity probe	0–100%	2.0m	Vaisala,HMP45C-L
Temperature probe	-45–60°C	2.0m	Vaisala, HMP45C-L
Barometric pressure sensor	600–1060 millibar	8.0m	Vaisala, CS105
Tipping bucket rain gage	0–15 mm	0.3m	TE525MM-L, R.M Young
Pyranometer (SW flux)	0–1200 W m ⁻²	1.5m	Kipp & Zonen, CM21
Pyrgeometer (LW flux)	0–700 W m ⁻²	1.5m	Kipp & Zonen, CG4
3-D Sonic anemometer		3.0m	Campbell, CSAT-3
Opened path infrared CO ₂ /H ₂ O analyzer		3.0m	Li-Cor, LI7500
Water content reflectometer	0–70 VV ⁻¹	5,10,20,40,80 cm	CAMPELL, CS616-L
Soil temperature profile	-50–70°C	2,5,10,20,50,80 <u>cm</u>	Hukseflux, STP01-L
Soil heat flux plate	-300–300 W m ⁻²	8 cm	Hukseflux, HFP01SC-L

2

3

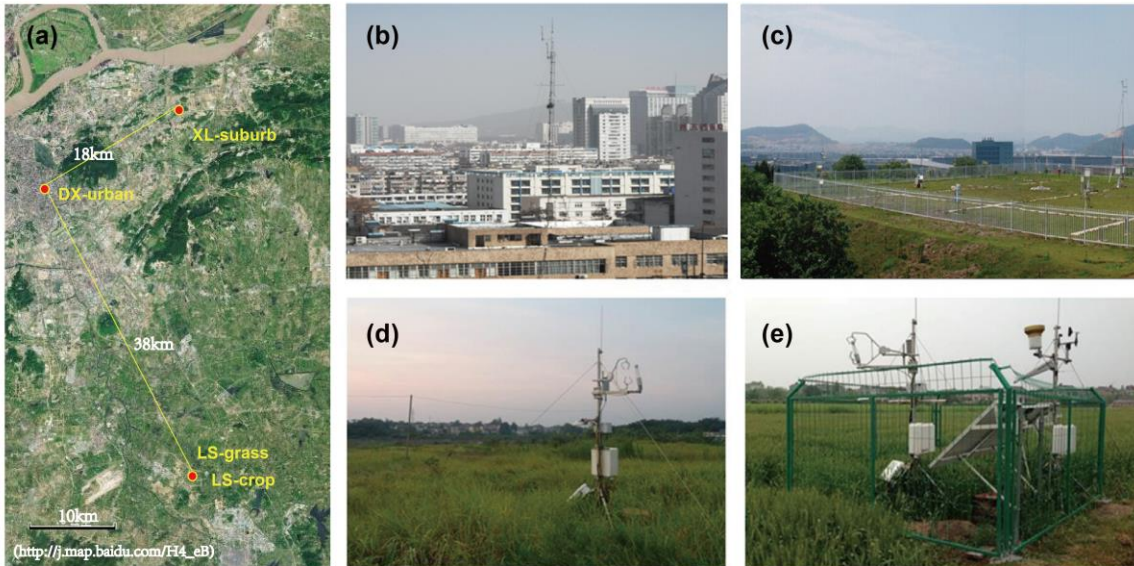
1 Table 2. Seasonal averages of Air temperature, surface temperature, and relative humidity at
 2 the four sites.

Site-name	LS-grass		LS-crop		DX-urban		XL-suburb	
	MAM	JJA	MAM	JJA	MAM	JJA	MAM	JJA
Ta(°C)	17.29	29.85	16.44	29.02	17.50	29.92	16.53	28.64
Ts(°C)	17.23	29.62	16.02	28.02	18.76	31.23	17.98	30.12
RH(%)	69.51	76.60	71.41	78.53	60.88	68.61	63.44	73.54

3

Micro-meteorological element	Site name	LS-grass		LS-crop		DX-urban		XL-suburb	
		MAM	JJA	MAM	JJA	MAM	JJA	MAM	JJA
average	Ta(°C)	17.29	29.85	16.44	29.02	17.50	29.92	16.53	28.64
	Ts(°C)	17.23	29.62	16.02	28.02	18.76	31.23	17.98	30.12
	RH(%)	69.51	76.60	71.41	78.53	60.88	68.61	63.44	73.54
Diurnal range	Ta(°C)	9.04	6.83	8.32	6.07	7.36	5.06	7.91	5.77
	Ts(°C)	14.51	11.67	12.22	7.77	10.64	9.26	16.19	12.46
	RH(%)	33.03	27.36	35.21	25.37	23.29	20.40	25.73	21.00

4



1

2

3 Figure 1. Location and surface types of four field sites at (b) DX-urban, (c) XL-
4 suburb, (d) LS-Grass and (e) LS-Crop in Nanjing.

5

6

7

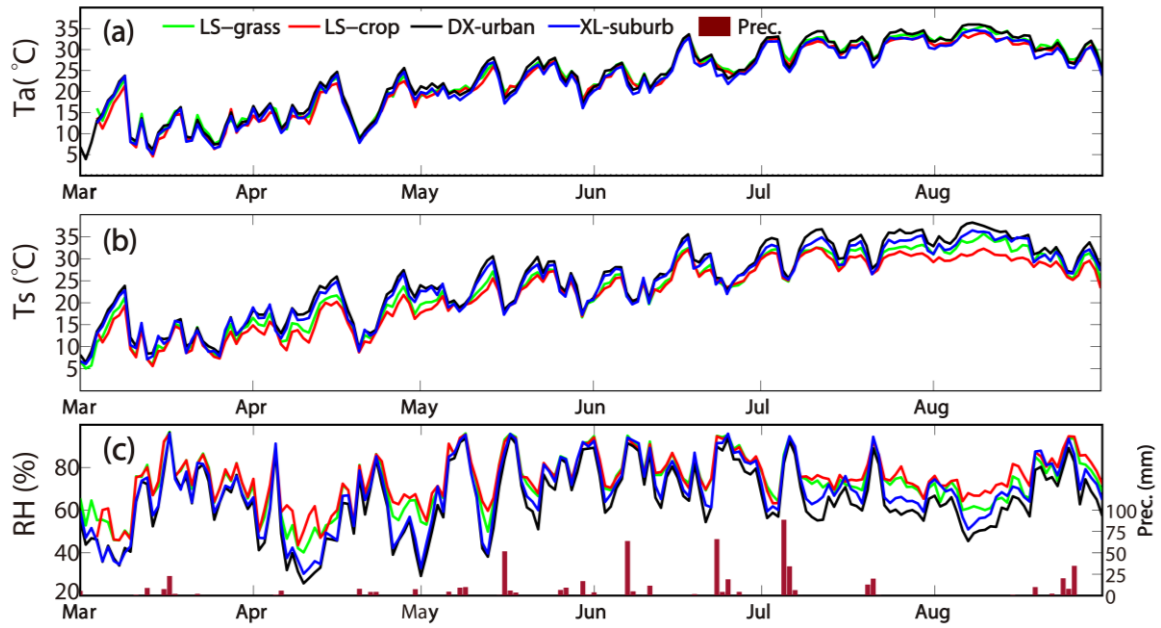
8

9

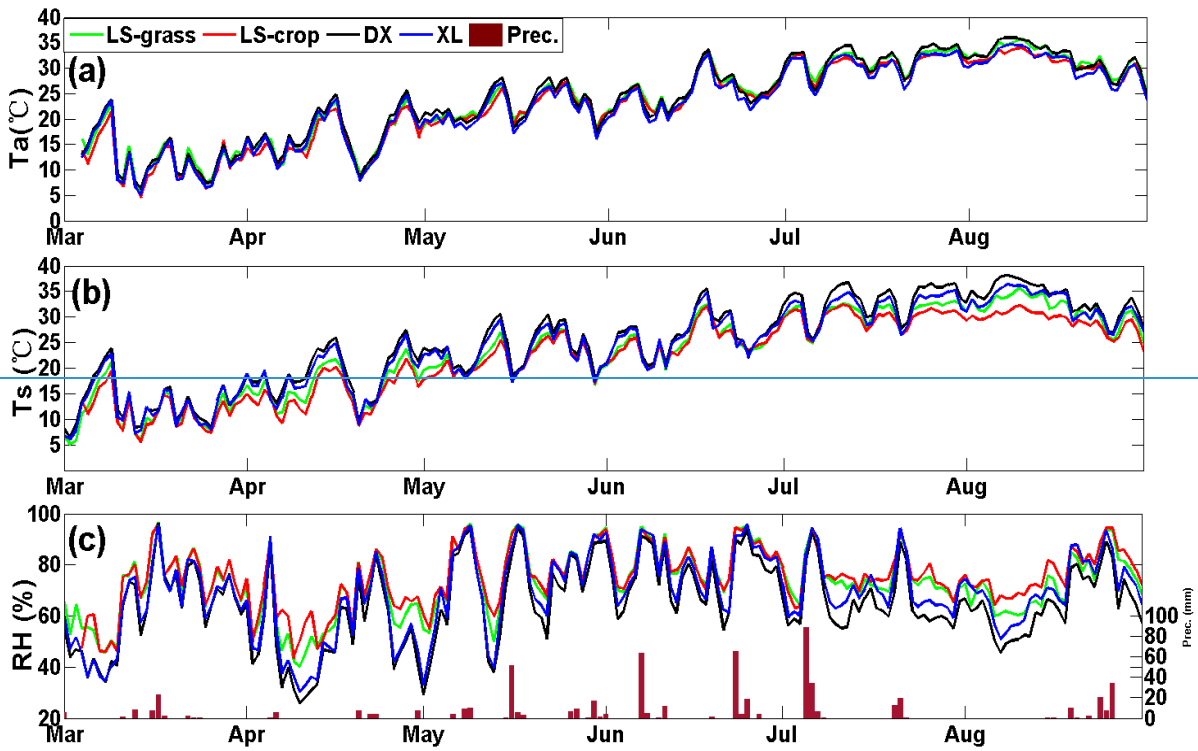
10

11

12



1

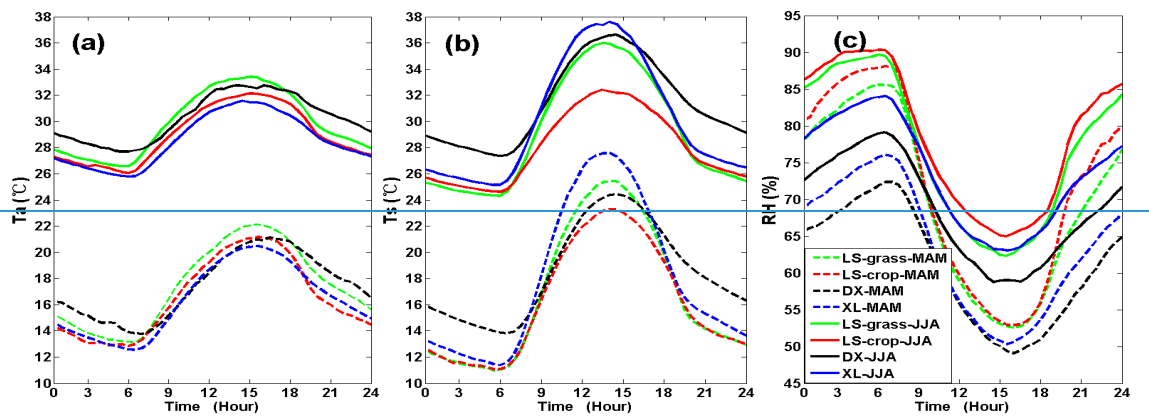
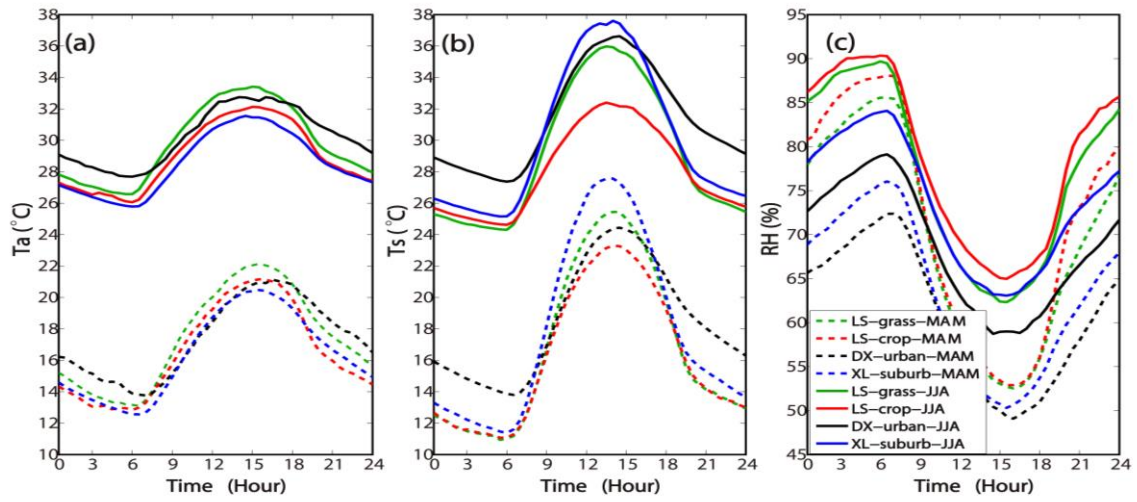


2

3

4 Figure 2. Daily variations of (a) air temperature, (b) surface temperature, and (c) relative
 5 humidity at the four sites in Nanjing from March to August, 2013.

6



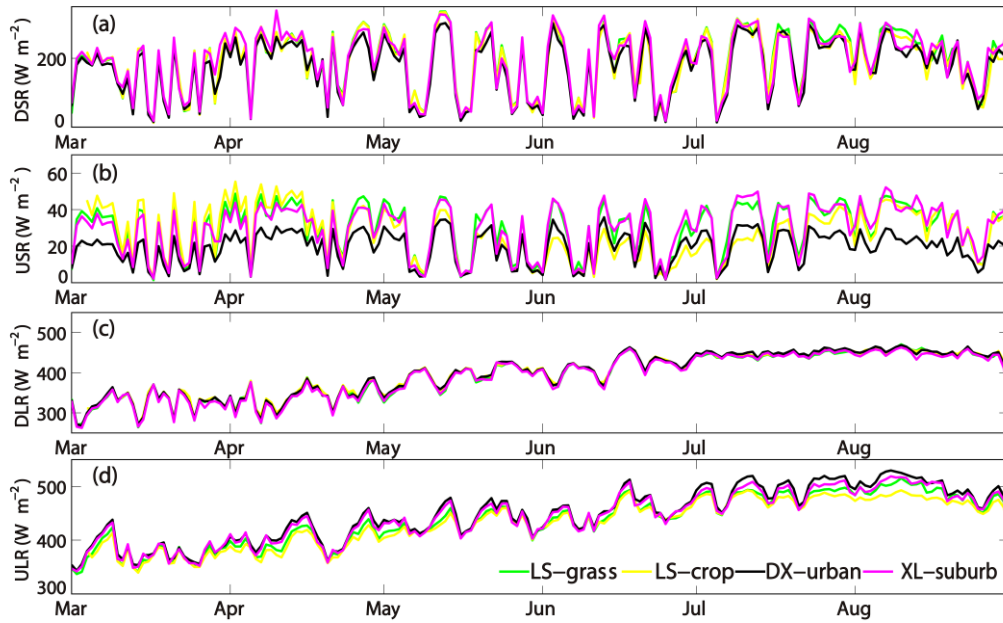
1

2

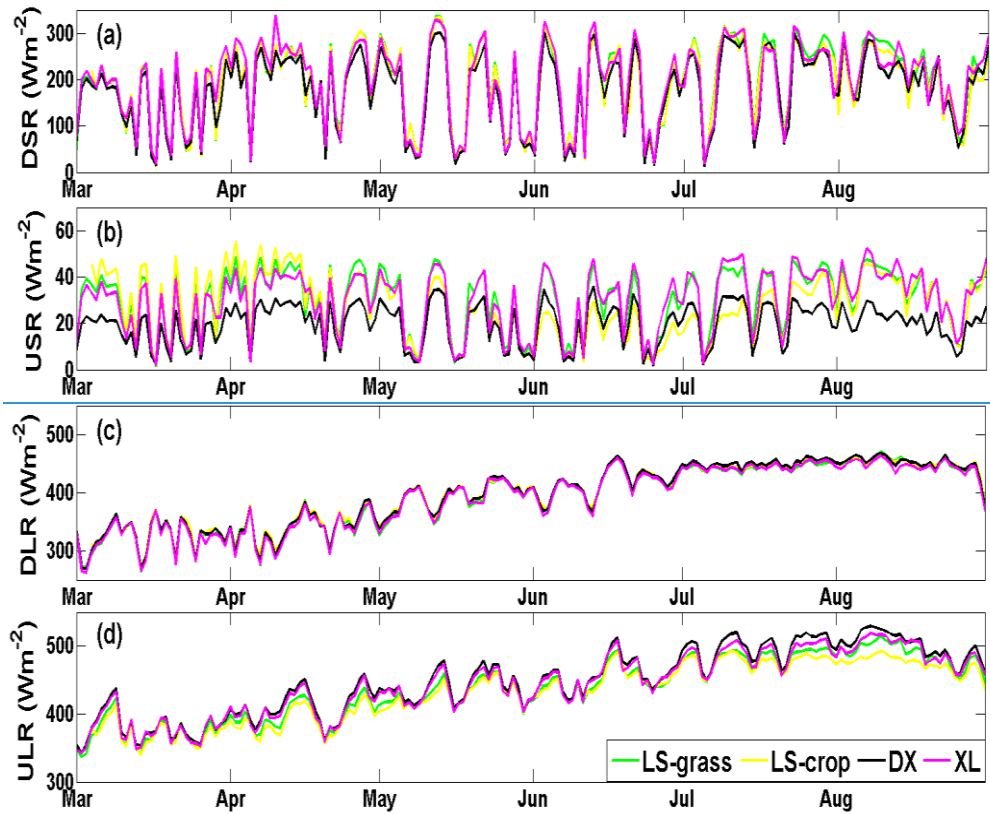
3

4 Figure 3. Diurnal variations of (a) air temperature, (b) surface temperature, and (c) relative
 5 humidity at the four sites in Nanjing in the spring and summer.

6



1

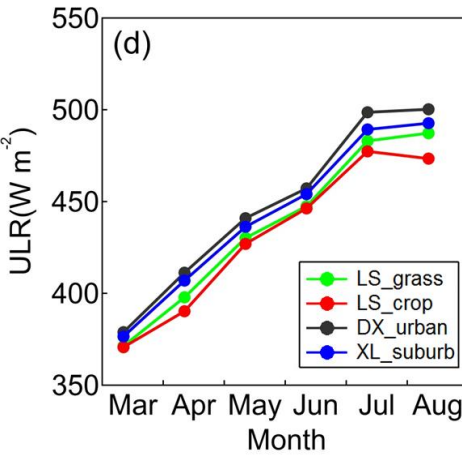
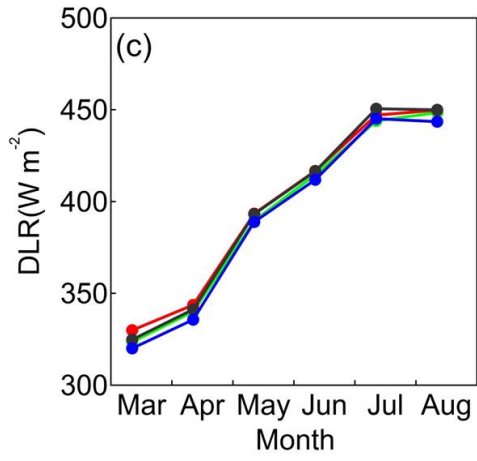
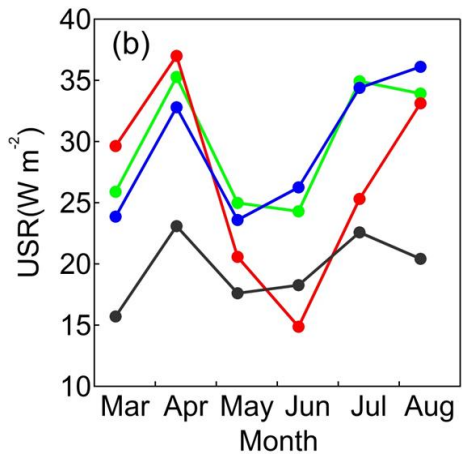
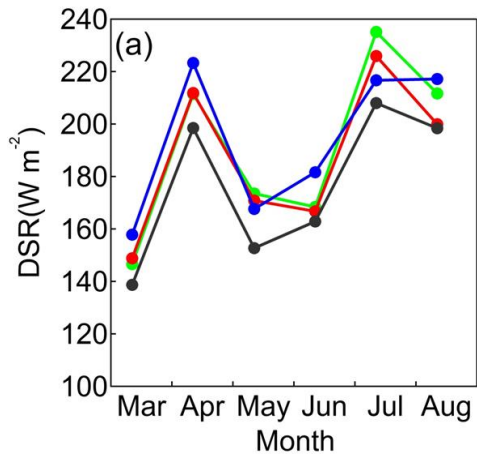


2

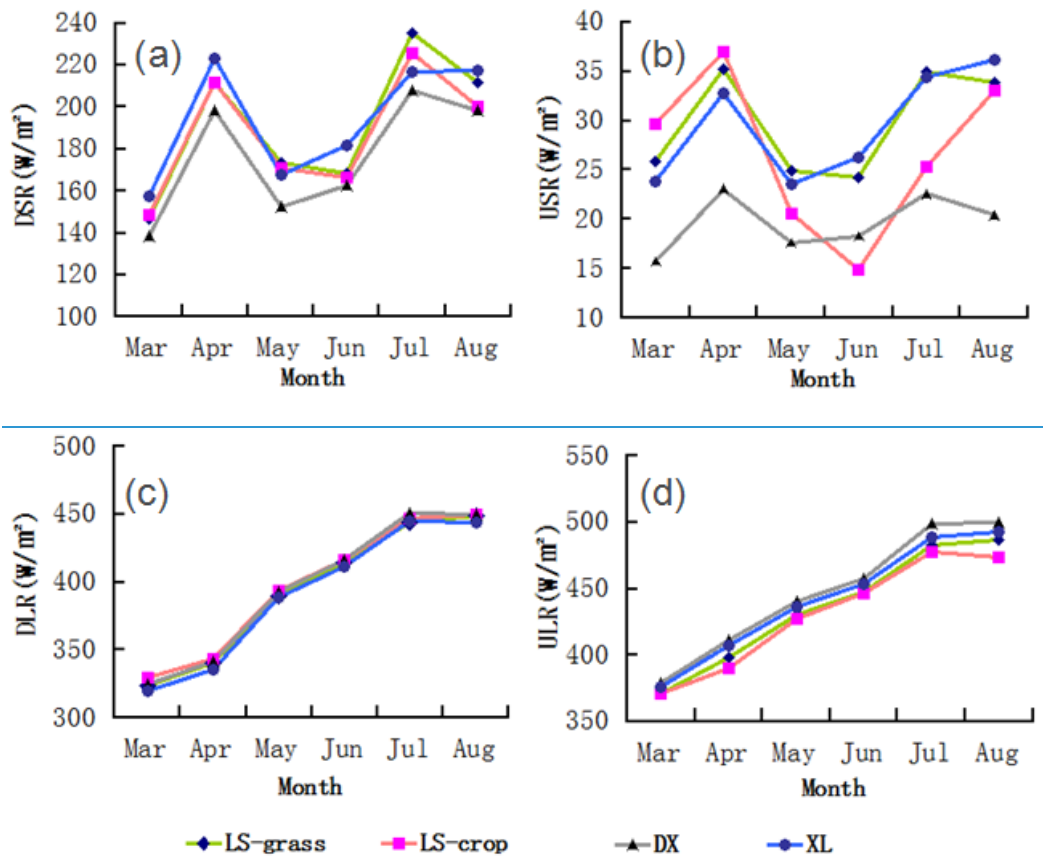
3

4 Figure 4. Daily variation of (a) downward shortwave radiation (DSR), (b) upward shortwave
 5 radiation (USR), (c) downward longwave radiation (DLR), and (d) upward longwave
 6 radiation (ULR) at the four sites in Nanjing.

7

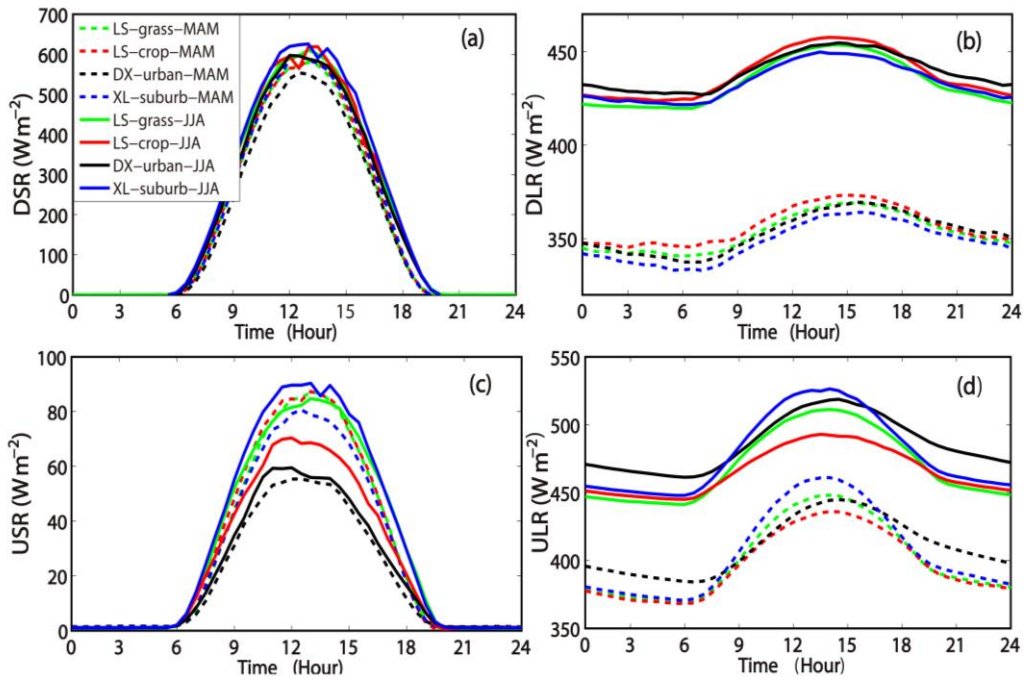


1

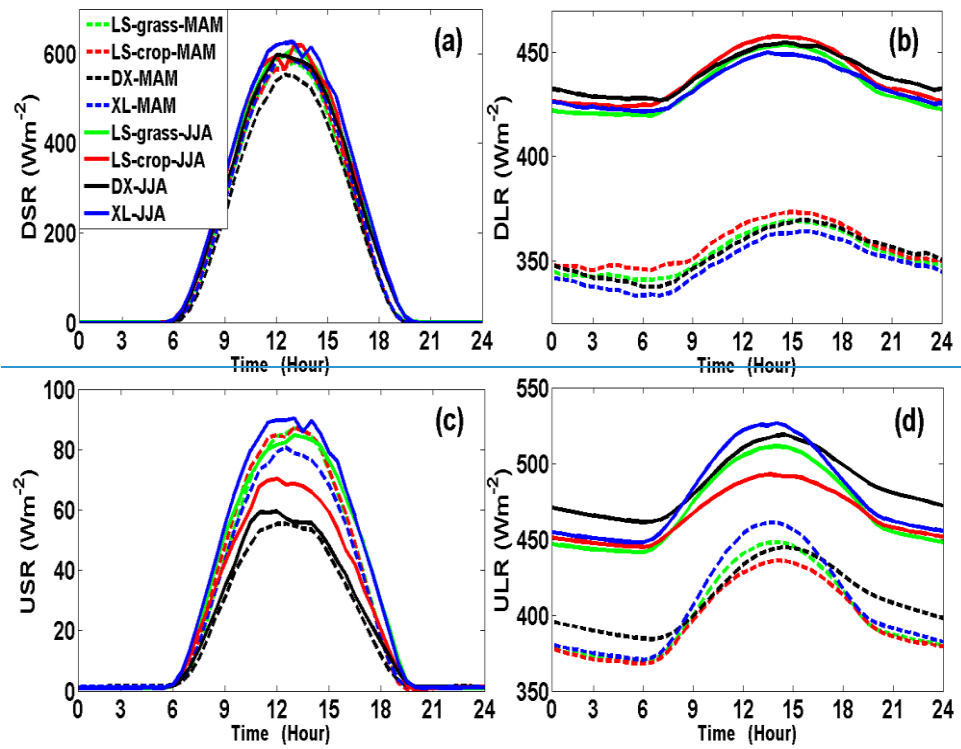


1
2
3
4
5
6

Figure 5. Monthly variation (a) downward shortwave radiation (DSR), (b) upward shortwave radiation (USR), (c) downward longwave radiation (DLR), and (d) upward longwave radiation (ULR) at the four sites in Nanjing.



1

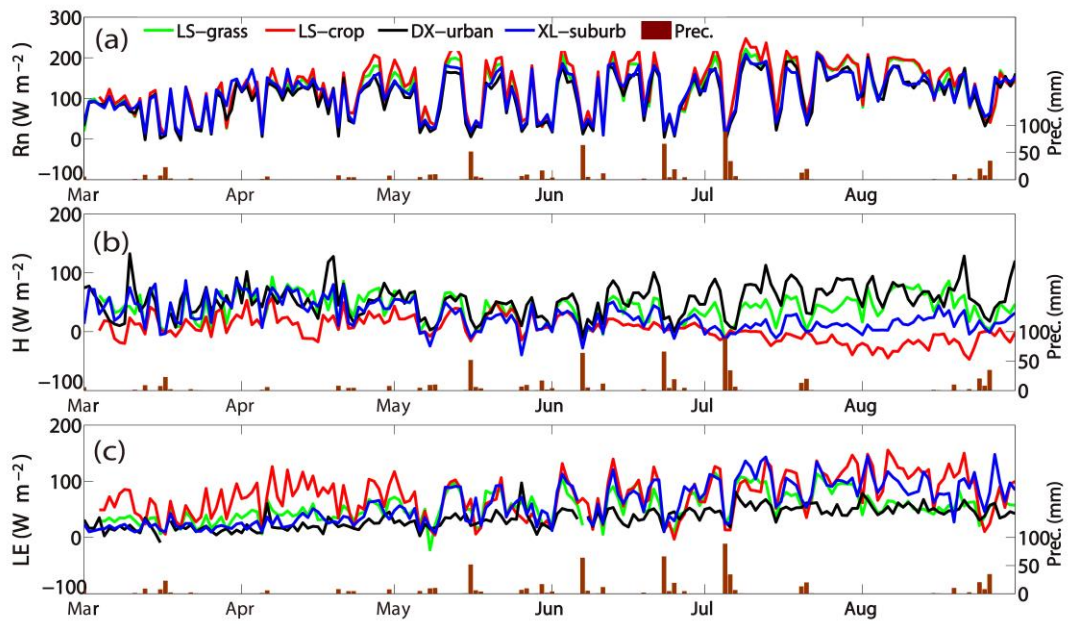


2

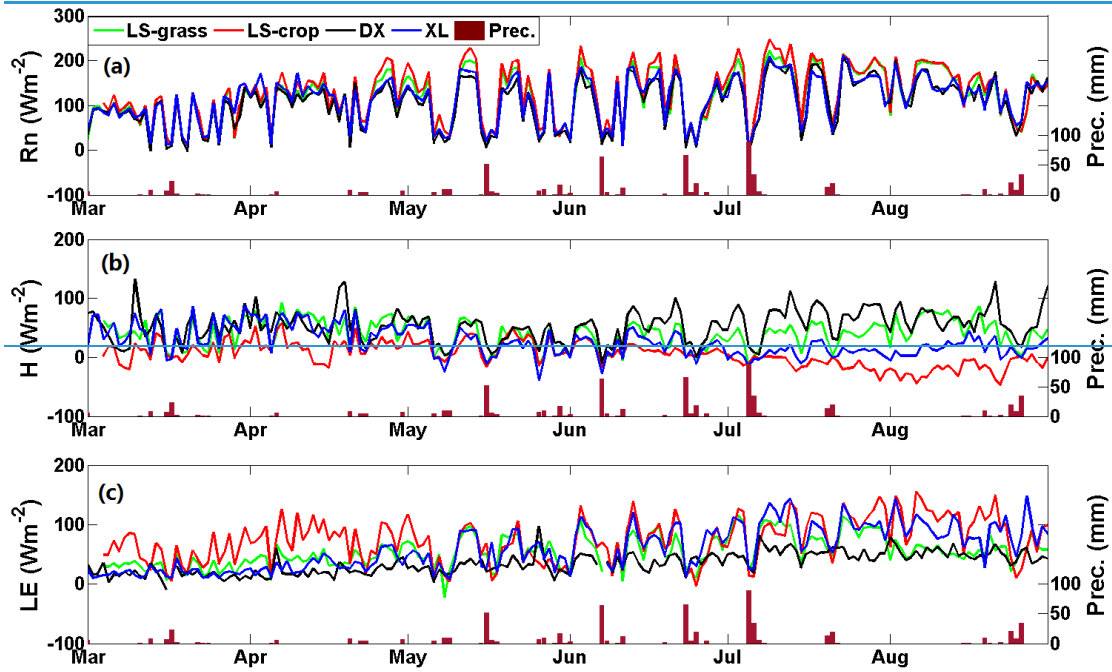
3

4 Figure 6. Diurnal variation of (a) downward shortwave radiation (DSR), (b) downward
 5 longwave radiation (DLR), (c) upward shortwave radiation (USR), and (d) upward longwave
 6 radiation (ULR) at the four sites in Nanjing.

7



1



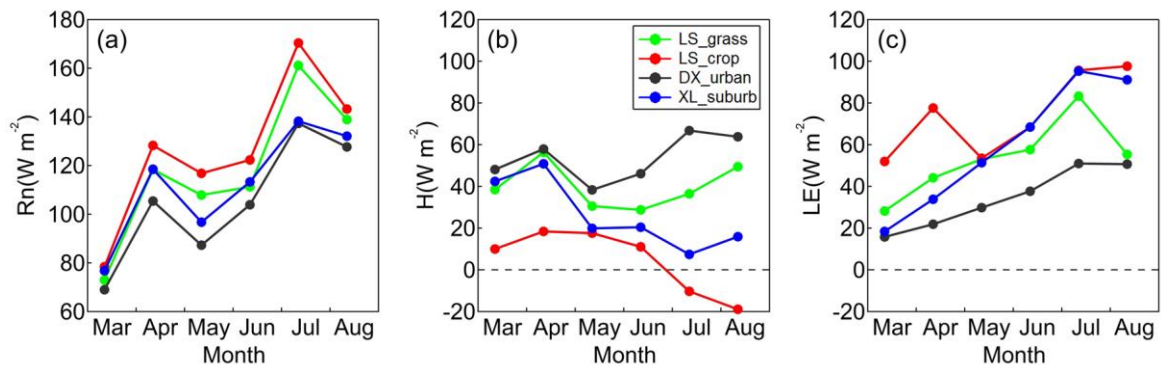
2

3

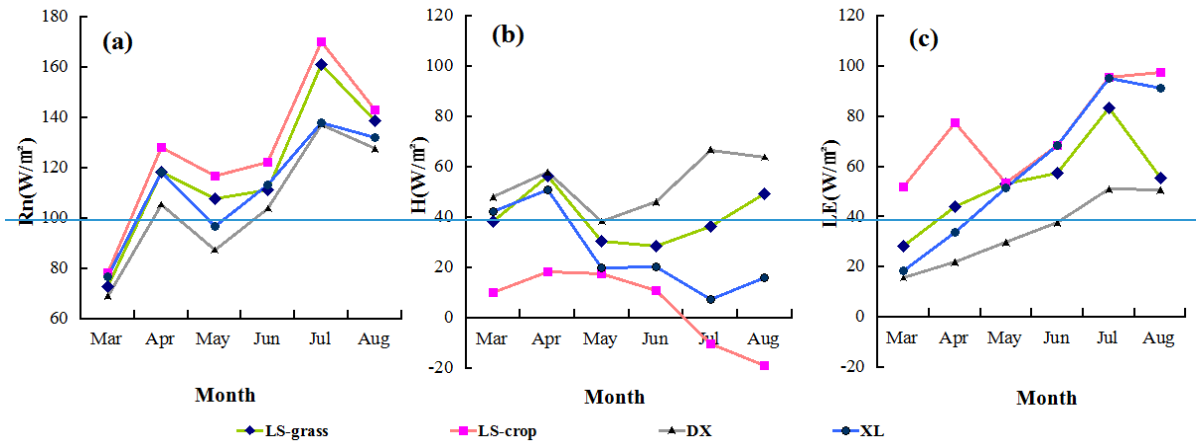
4 Figure 7. Daily variations of (a) net radiation, (b) sensible heat flux, (c) latent heat flux at the
 5 four sites in Nanjing from March to August, 2013.

6

7



1

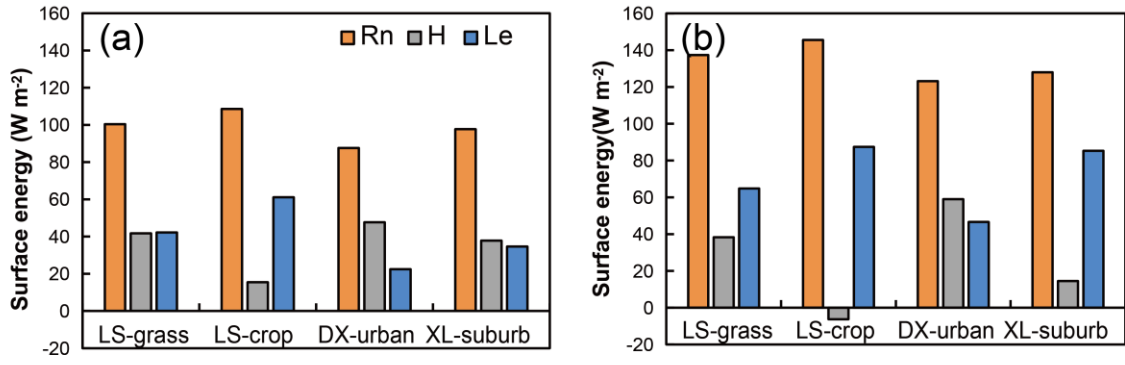


2

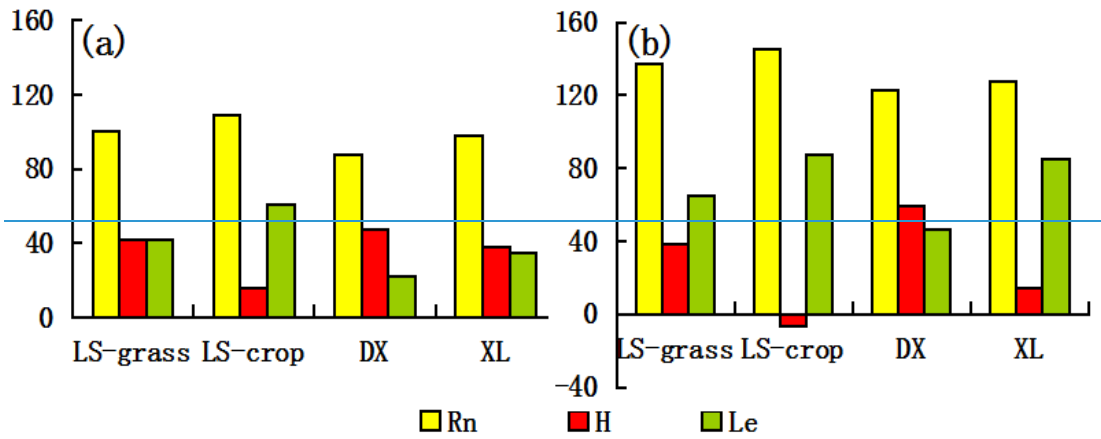
3

4 Figure 8. Monthly variation of (a) net radiation, (b) sensible heat flux, (c) latent heat flux at
 5 the four sites in Nanjing from March to August, 2013.

6



1



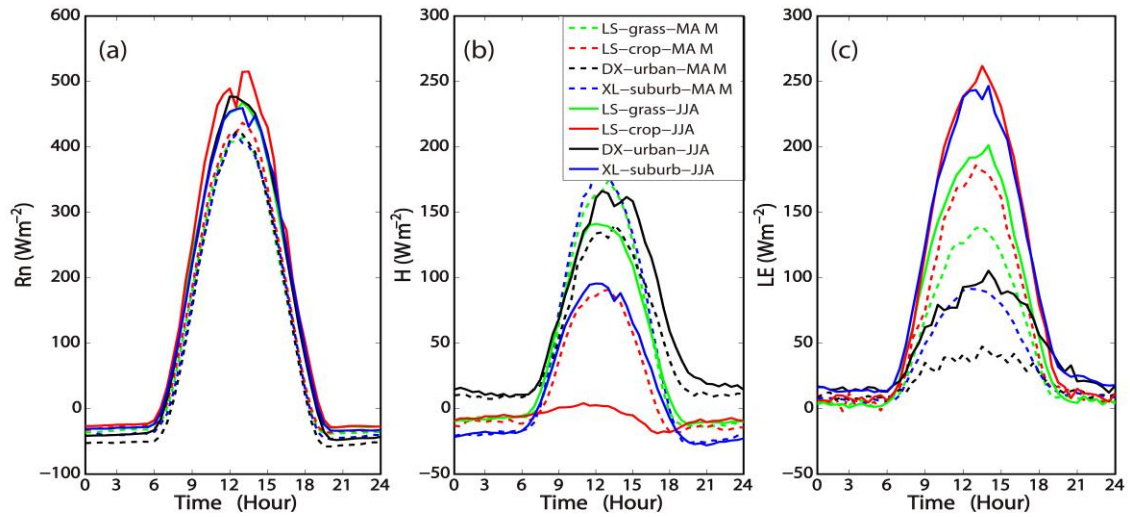
2

3

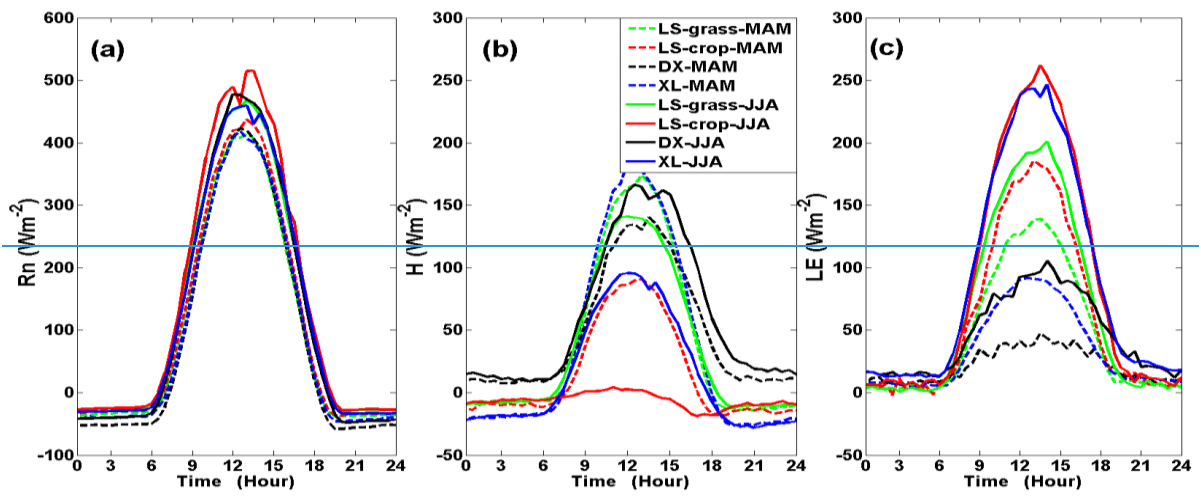
4 Figure 9. Seasonal average distribution of surface energy for the (a) spring and (b) summer at
 5 the four sites in Nanjing.

6

7



1

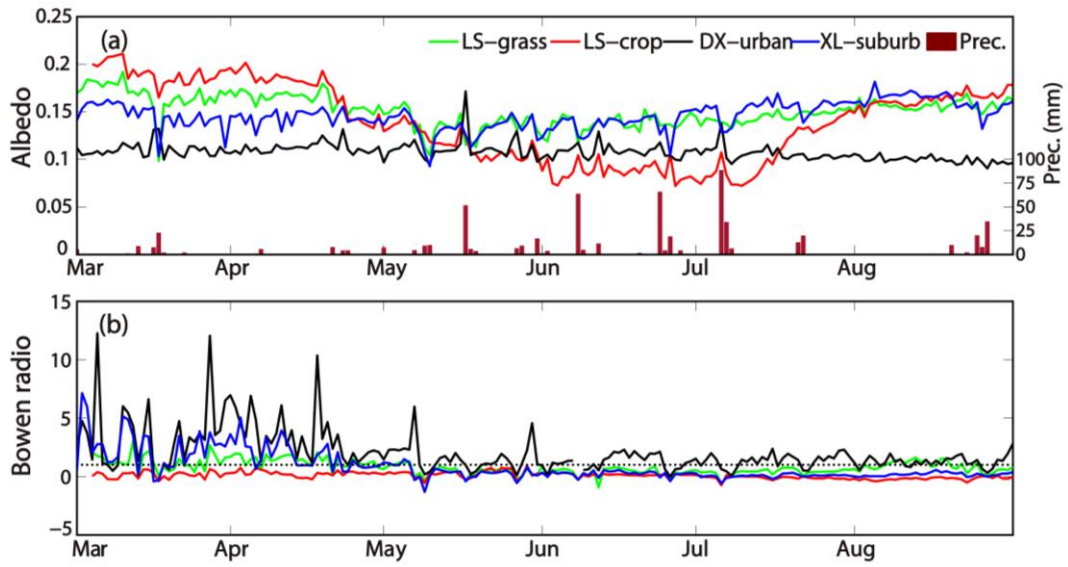


2

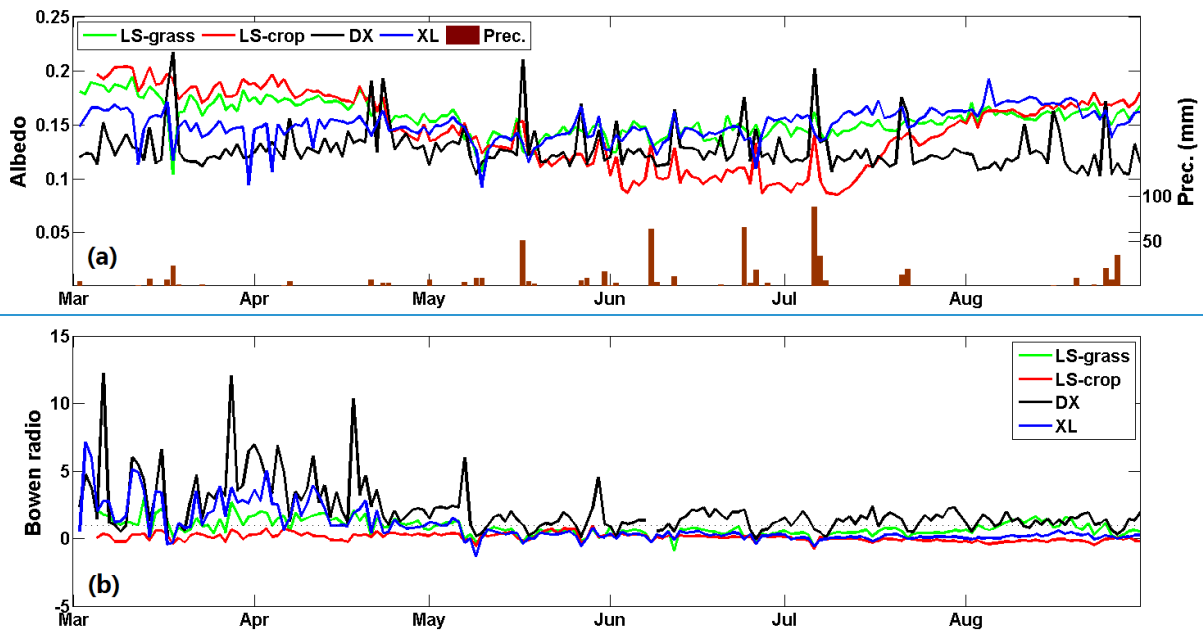
3

4 Figure 10. Diurnal variation of (a) net radiation, (b) sensible heat flux, (c) latent heat flux at
 5 the four sites in Nanjing from March to August, 2013.

6



1



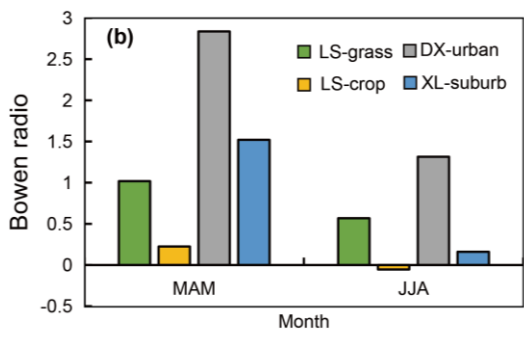
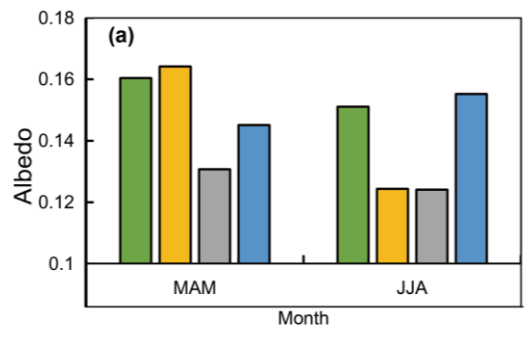
2

3

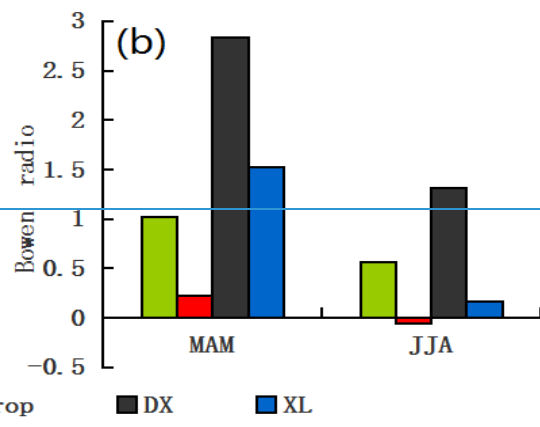
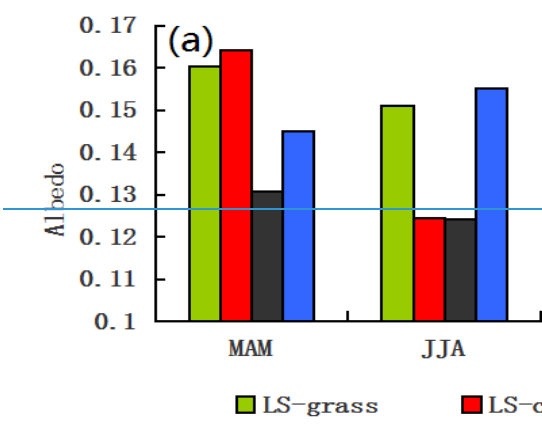
4 Figure 11. Daily variation of (a) albedo and (b) Bowen ratio at the four sites in Nanjing from
 5 March to August, 2013.

6

7



1

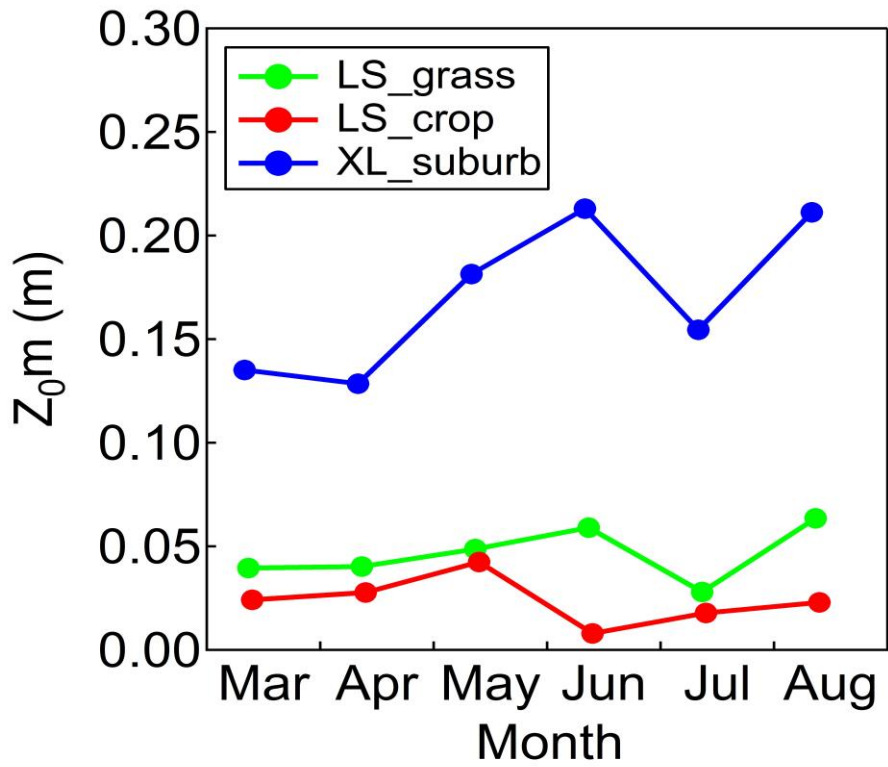


2

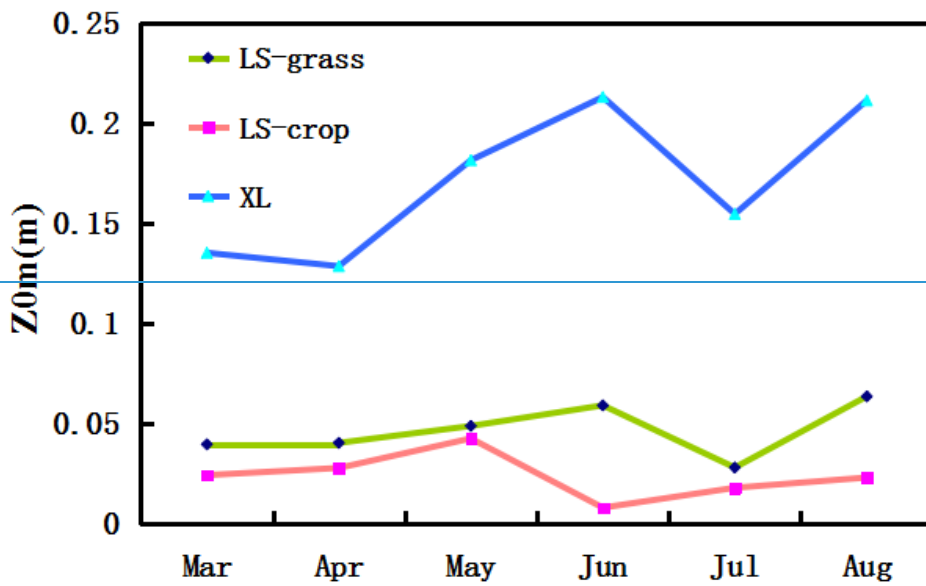
3

4 Figure 12. Seasonal averages of (a) albedo and (b) Bowen ratio for the spring and summer at
 5 the four sites in Nanjing.

6



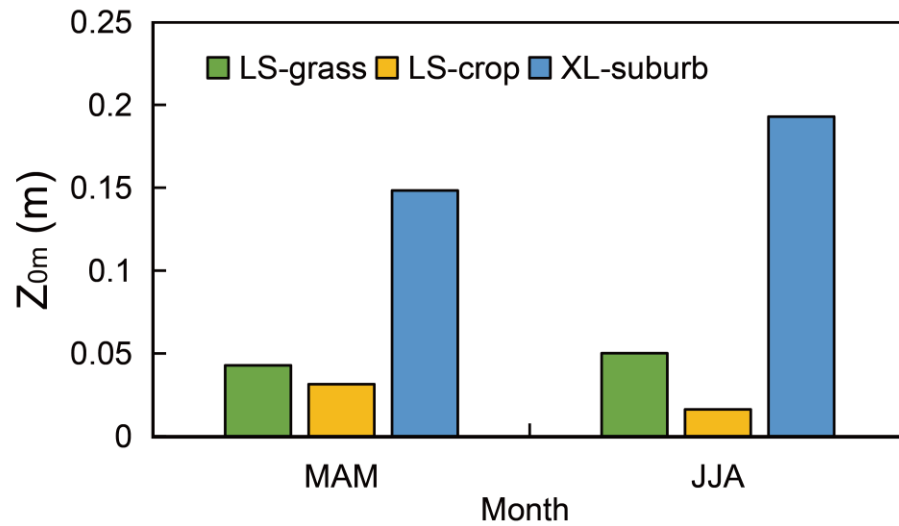
1



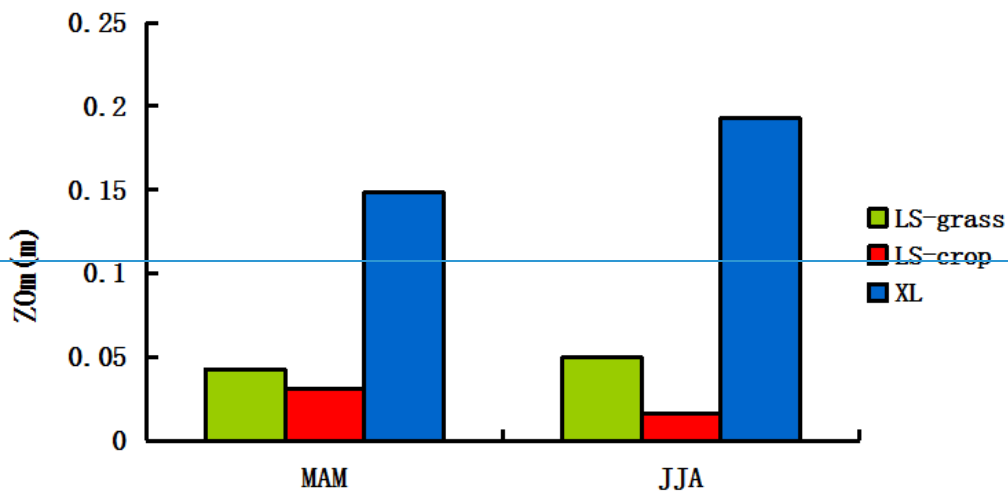
2

3 Figure 13. Monthly variations of surface roughness length at the three sites in Nanjing from
 4 March to August, 2013.

5



1



2

3 Figure 14. Seasonal averages of surface roughness length at the four sites in Nanjing for the
 4 spring and summer of 2013.